Efficiency Mapping of Single Phase Induction Machines for Motoring and Generating Operations

by

Mahima Gupta

A dissertation submitted in partial fulfillment of
the requirements for the degree of

Master of Science

(Electrical and Computer Engineering)

at the

UNIVERSITY OF WISCONSIN–MADISON

2015

APPROVED BY:

Advisor Signature: 

Advisor Title: Professor

Date: 21 August 2015

ACKNOWLEDGMENTS

First and foremost, I would like to express my sincere gratitude to my supervisor, Dr. Giri Venkataramanan who has been a very supportive and encouraging mentor. His approach towards tacking problems has shown me how to analyze, deduce and solve a variety of problems. Whenever I have been stuck, he has guided me along the path.

I would also like to extend my sincere thanks to the Wisconsin Electric Machines and Power Electronics Consortium (WEMPEC): Ray Marion, Helene Demont and the rest for all of their assistance; the sponsors for their continued support; the faculty for their in-depth knowledge and expertise; the symposiums and all the WEMPEC students for their friendship and advice.

Lastly I would like to thank my family and friends for their love and support.

CONTENTS

LIST OF TABLES

LIST OF FIGURES

ABSTRACT

Single Phase Induction Machines form the work-horse of various fractional-power domestic and agricultural applications such as vacuum cleaners, fans, water pumps etc. They are often designed to be simple, rugged and low-cost. This work is aimed at using these single-phase induction machines for wider applications.

A majority of single-phase induction machines are capacitor-start type of induction machines. These machines have two-stator windings in space and time quadrature. One of these windings is used only to start the machine. The possibility of using this passive winding as an active winding, functional throughout the machine operation, by simply retrofitting a run capacitor, has been discussed in this work. Consequently, this two-phase winding machine has been proposed to be used as a wind turbine generator coupled with power electronics. The suggested dc-link inverter single-phase induction machine system can be an economical generator system to provide for fractional horsepower applications as compared to the conventional and expensive permanent magnet generators.

Computer simulation results have been used to confirm the analytical results of the proposed two-phase machine and wind-turbine generator system. Results of some preliminary experiments from a laboratory prototype of the two-phase motor have been presented.

1 INTRODUCTION

Induction motors are the most popular and widely used type of AC motors in the world. Most of the fractional horsepower applications use single phase induction motors (SPIMs) whereas for integral horsepower applications, polyphase induction machines are popular. Hence, for general purposes in homes, offices, small factories, single phase induction machines are more economical. The power requirement for these applications are small, which can be easily met by single phase power supply system. Additionally, single phase motors are simple in construction, cheap in cost, reliable and easy to repair and maintain. Due to all these advantages the single phase induction motor finds its application in vacuum cleaners, fans, washing machines, centrifugal pump, blowers, washing machines, etc. [9].

Like any three phase induction machine, SPIMs work on the principle of current induction in the rotor bars due to alternating currents in the stator. However, SPIMs are not self-starting. These machines utilize various starting arrangements giving rise to many types of SPIMs. This chapter discusses the working principle and various types of SPIMs in detail [1, 13, 14, 15]. The equivalent q-d circuit model of the induction machine has also been introduced in this chapter.

1.1 Working principle of Single Phase Induction Machines

A single phase induction machine is derived from a two phase induction machine arrangement. Once the concept behind a two-phase arrangement is developed, it can be extended to single-phase supply machines.

Figure 1.1 represents the winding arrangement of a two phase machine.

The machine is shown to have two phases, Phase 1 and Phase 2 respectively. The windings of the two phases are 90° out of phase with each other in space. Furthermore, they are fed with a power supply system that are also fed with currents that are 90° out of phase with each other in time, shown in Figure 1.1a, marked by four instants of time, 1 through 4. The resultant instantaneous fields which are set up at these instants of time due to the currents in the two stator phases are illustrated in Figure 1.2 [5, 10].

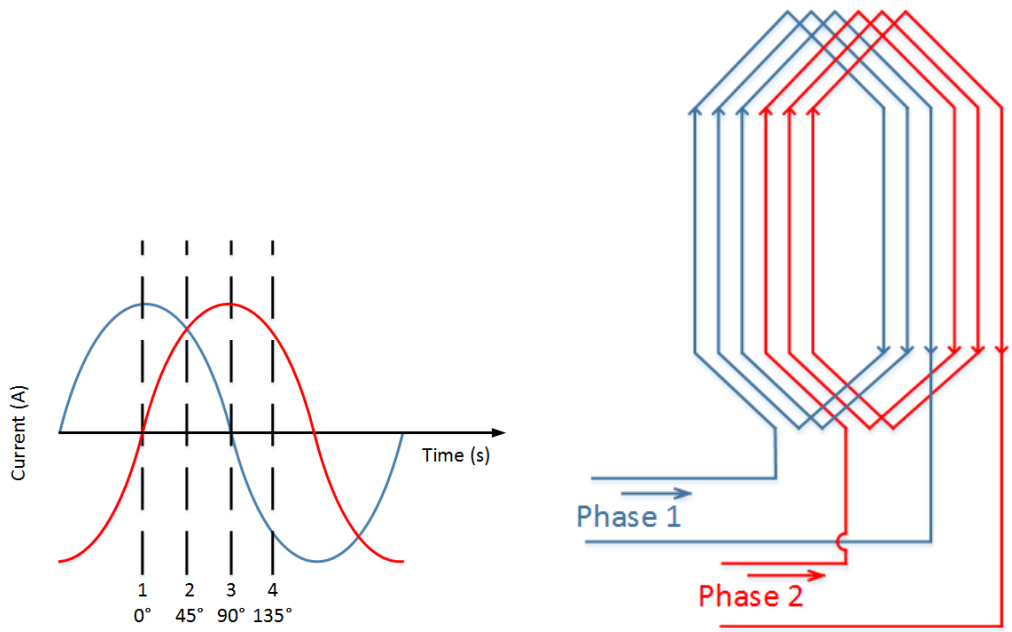

(a) Two Phase Sinusoidal System (b) Machine Windings

Figure 1.1: Illustrations of a Two Phase Machine

At instant 1 i.e 0° angle, Phase 1 is maximum while Phase 2 is zero. Hence, it can be seen that slots 1-3 have currents flowing out of the page while slots 7-9 have return path for these currents. Slots 4-6 and slots 10-12 have zero currents in them. Application of right hand rule gives the flux direction during this instant of time. Similarly, at instant 2 i.e. 45° angle, Phase 1 and Phase 2 have currents of equal magnitude and angle. Similar

application of right hand rule shows that the air-gap flux is same as time instant 1 but is shifted by 45° in space.

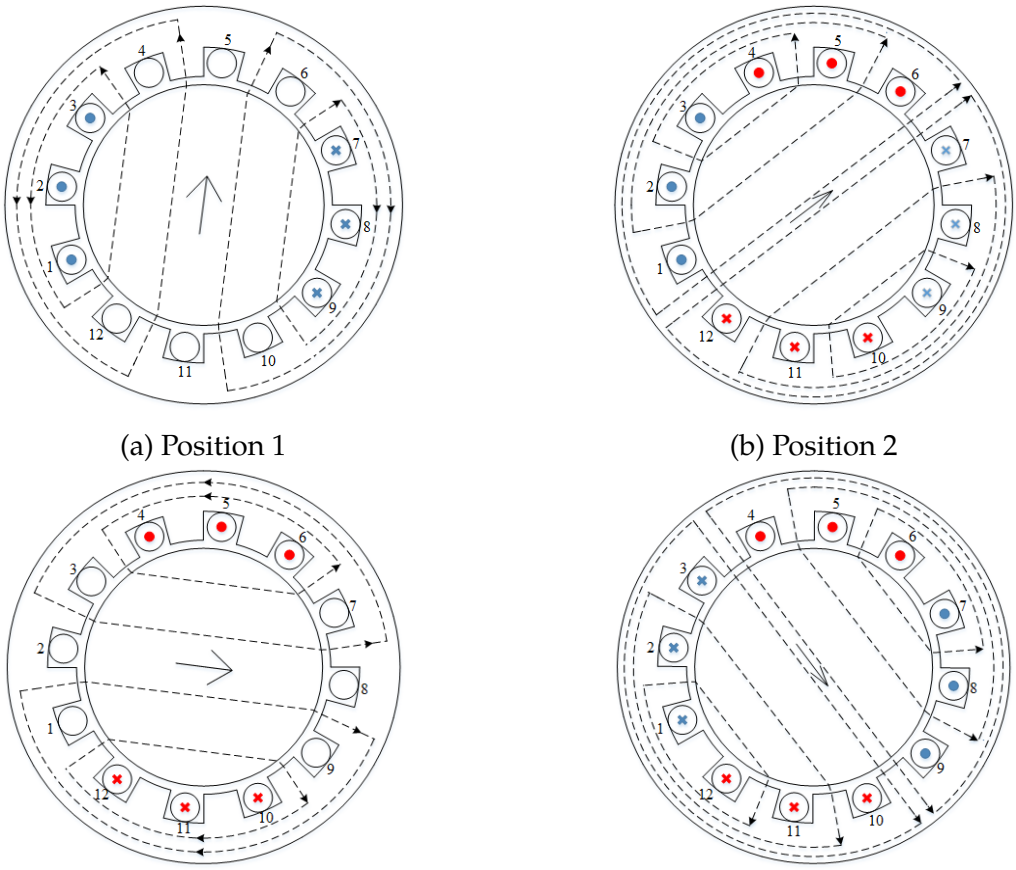

(a) Position 1

(b) Position 2

(c) Position 3

(d) Position 4

Figure 1.2: The rotating field set up in a two-phase Machine

Instant 3 is similar to instant 1 except now Phase 2 has the maximum current while Phase 1 has zero current. The air-gap flux in this case is 90° shifted from instant 1 or 45° shifted from instant 2. Instant 4 has Phase 1 with current in negative direction. Hence, slots 1-3 have currents flowing into the page. Phase 2 has positive current direction hence slots 4-6 show current direction out of the page. The air-gap flux in this case is 135°

shifted from instant 1. Similar analysis can be done for one complete cycle. It can be seen from this analysis that in a two-phase machine, rotating flux is generated which covers one complete 360° cycle in every 50/60 Hz cycle.

Hence, the conditions necessary to set up a rotating field in a two-phase machine are: (1) the two windings of the motor have to be located 90 electrical degrees apart in space. (2) the excitation currents in the two phases have to be displaced by 90 degree in time.

While, these conditions appear necessary to realize a rotating magnetic field, they are not necessary to develop a motoring interaction through induced currents in a suitably designed rotor placed in the rotating magnetic field. A single phase induction motor may be realized where one of the two phase windings and the power supply is omitted! To be sure, while such an arrangement may realize torque production, it can be shown that single phase motors are not self-starting. In general, two theoretical approaches described further are widely used in order to analyze torque production in single-phase induction machines.

1.1.1 Cross-field theory

In case of a single phase winding at the stator, the shape and direction of the field will be as shown in Figure 1.3. Assuming that the rotor is in motion and is moving in the clockwise direction, voltage will be generated in the rotor bars which will be as shown in the figure (owing to Fleming's three-finger rule).

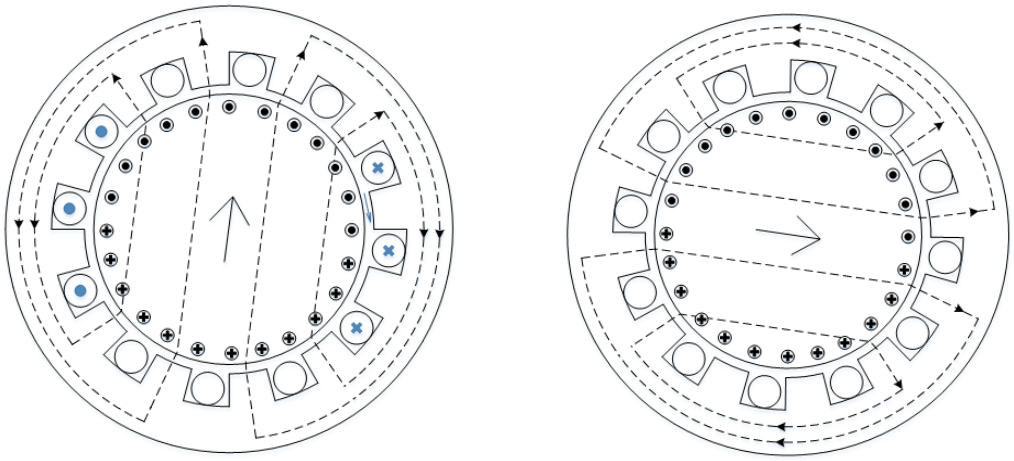

(a) Stator field and the rotational induced voltages in the rotor

(b) Magnetic field set up by currents in the rotor (cross field)

Figure 1.3: Cross field theory

These rotor currents set up a field as shown in Figure 1.3b. The axis along which this field is set up is called cross-field axis. This axis is the direction along which the field is set up by the currents which are induced by cutting the main-axis flux. If the rotor is at stand-still, the cross field currents will be zero.

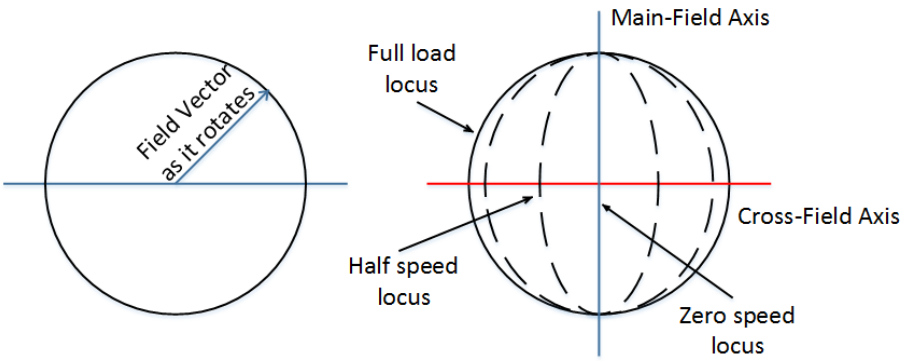

Figure 1.4: Comparison of Rotating Fields in a polyphase machine and a single-phase machine at different rotor speeds

Hence, it can be seen from Figure 1.4 that the net field in a single-phase machine tends to be elliptical, when the rotor is in motion.

1.1.2 Revolving-field theory

The air-gap flux vector in case of a single-phase induction machine is a stationary vector which merely pulsates in magnitude. This vector can hence be resolved into sum of two uniformly rotating vectors, equal in magnitude and rotating opposite in direction (Figure 1.5).

From this, Ferraris [15] deduced that the single-phase induction machine can have the same characteristics as two polyphase motors rotating in opposite direction. The net shaft torque would hence be the algebraic sum of these two torques at any speed. These two torques are called forward and backward torque (Figure 1.6)

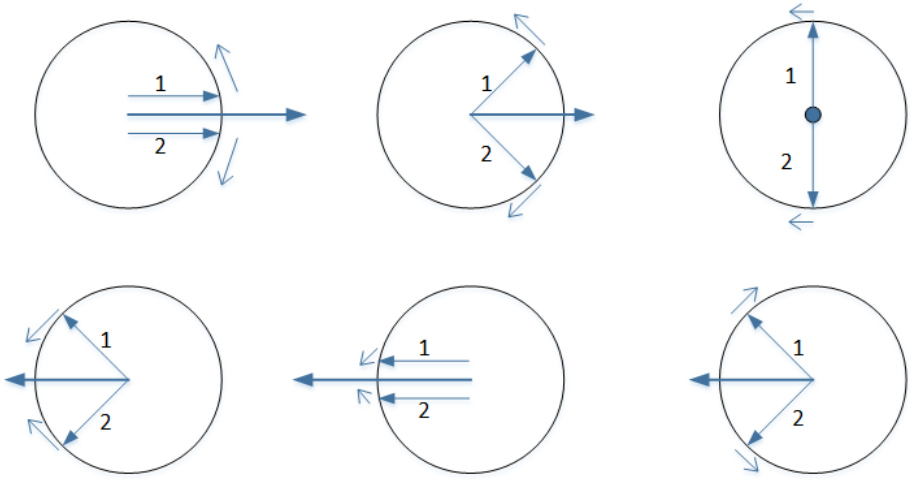

Figure 1.5: Illustration of vector fields in the Revolving-field theory

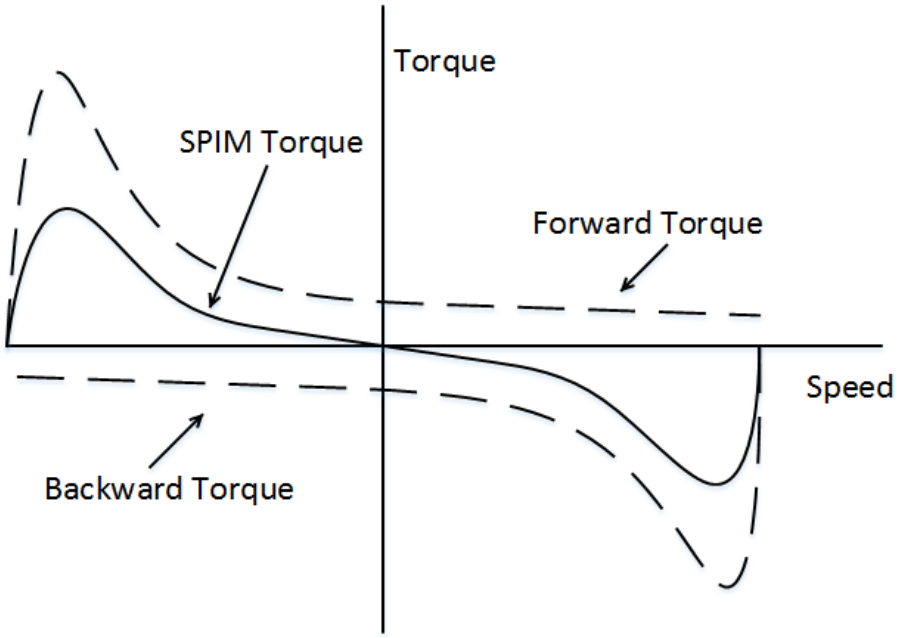

Figure 1.6: Ferraris Method of Explanation of Torque-Speed curve of a single phase induction machine

The cross-field theory appeals to some, the revolving field theory to others. Both theories explain most of the known and demonstrable facts. The revolving field theory is often useful for equivalent circuit analysis.

1.2 Types of Single Phase Induction Machines

Since the single phase induction machines are not self-starting, special starting arrangements have to be made. This gives rise to various types of SPIMs which are discussed in this section.

1.2.1 Split-phase Induction Motors

Split-phase induction machines were the first kind of SPIMs built. These machines can be defined as those SPIMs which are equipped with an

auxiliary winding, displaced in magnetic position from and connected in parallel with the main winding without using any other impedance in series or parallel (Figure 1.7).

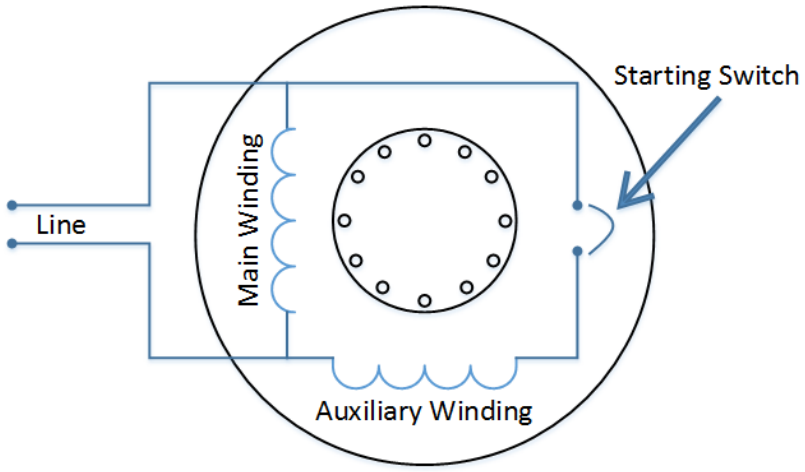

Figure 1.7: Schematic representation of a split-phase Induction Machine

Along with an auxiliary winding, the machine has a centrifugally operated starting switch which disconnects the auxiliary winding from the machine once the machine reaches 75-80% of its full load speed.

As was developed in the previous chapter, in order to obtain a rotating air-gap field, the two windings of the machine have to be placed 90 degrees apart in space and time. In this case, the space criteria is easily met.

If the impedance of the auxiliary winding is higher, and different in angular value, the current in the winding will be lower and displaced in time as compared to the main winding. Thus the current in the two windings would be displaced somewhat in time (although much less than 90 degrees) resulting in a moderately high starting torque. Once the machine reaches its about 75-80% of the rated speed, the centrifugal switch disconnects the auxiliary winding from the machine.

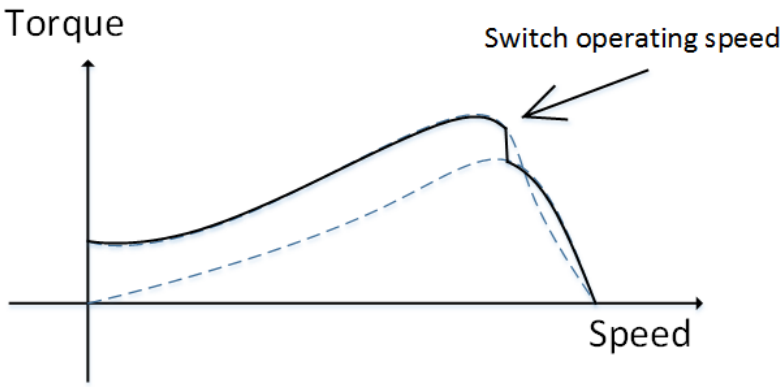

Figure 1.8: Torque-speed curve of a typical split-phase Induction Machine

The auxiliary windings are usually made up of smaller size of copper wire which saves upon weight and space for the main winding of the machine.

1.2.2 Capacitor-start Induction Motors

Capacitor-start induction machines can be defined as those SPIMs which are equipped with an auxiliary winding, displaced in magnetic position from and connected in parallel with the main winding using a capacitor in series with it (Figure 1.9).

The main and auxiliary winding are displaced by 90 degrees in space. By choosing the right value of capacitance, very good displacements in time domain can also be attained (of the order of 90 degrees). It can been intuitively seen that the locked rotor torque in this type of machine can be much higher that the split-phase machine.

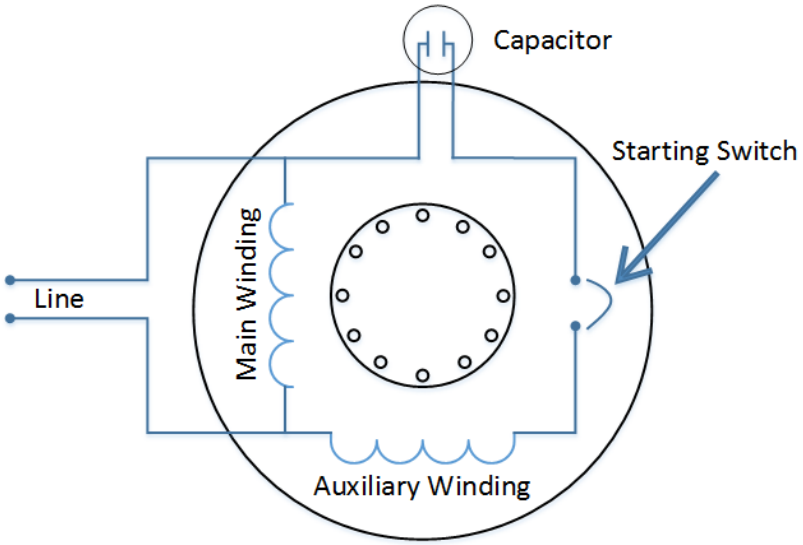

Figure 1.9: Schematic representation of a capacitor-start Induction Machine

Similar to the split-phase machine, once the rotor reaches about 75-80% of the rated speed, the centrifugal switch disconnects the auxiliary winding from the machine. The auxiliary windings of the capacitor-start motor usually contains more copper than the auxiliary winding of the split-capacitor motor.

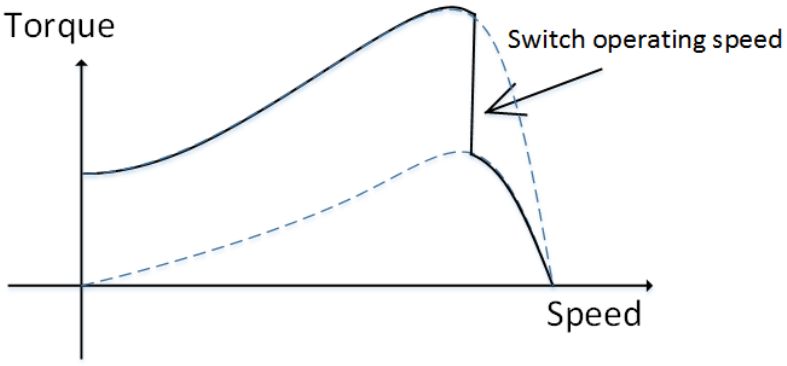

Figure 1.10: Torque-speed curve of a typical capacitor-start Induction Machine

1.2.3 Permanent-split capacitor Induction Motors

Permanent split induction machines can be defined as those SPIMs which are equipped with an auxiliary winding, displaced in magnetic position from and connected in parallel with the main winding using a run capacitor in series with it (Figure 1.11). The machine does not have any switch to disconnect the auxiliary winding during normal operating conditions.

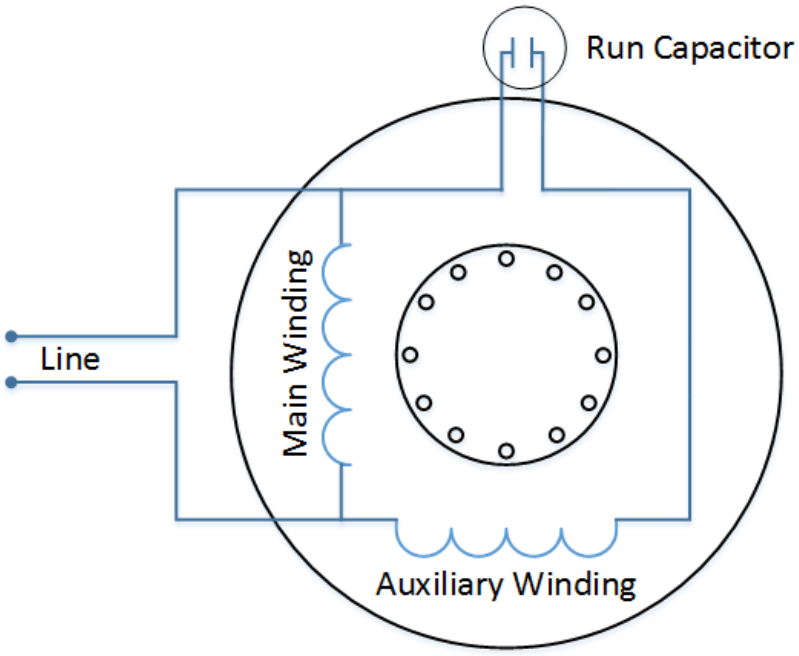

Figure 1.11: Schematic representation of a permanent-split Induction Machine

These type of motors have low starting torque. These machines are typically used for special-duty applications.

1.2.4 Two value Induction Motors

A two value capacitor motor is the form of a motor that starts with one value of capacitor in series with the auxiliary winding and runs with a

different value. This change between the capacitors is automatic with the help of the centrifugal switch (Figure 1.12).

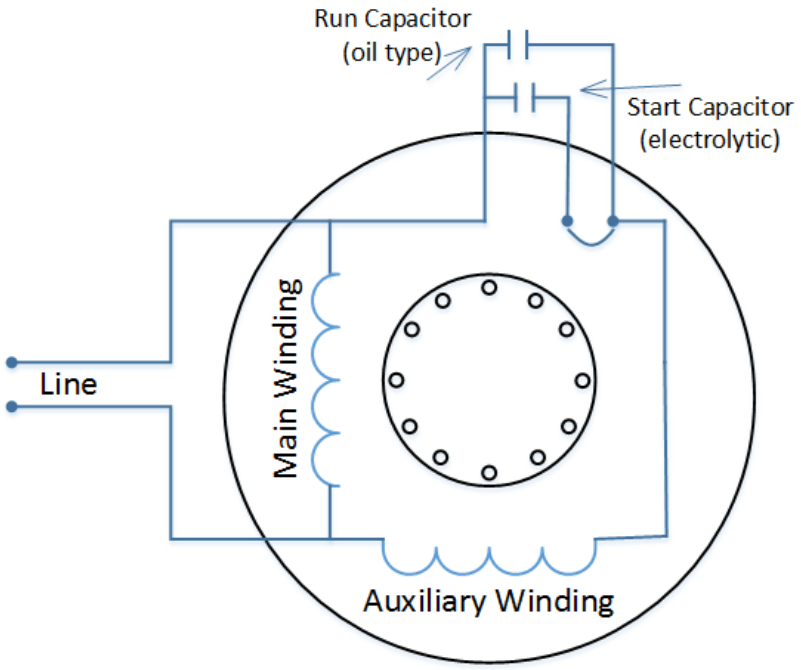

Figure 1.12: Schematic representation of a two-value Induction Machine

The start capacitor leads to a high starting torque. The effect of addition of a run capacitor is as follows: (1) increases the breakdown torque (2) improves the machine full load efficiency (3) improves the operating power factor (4) reduces the full-load running current (5) reduces noise under full load running conditions.

All these advantages are a result from the presence of a true rotating field due to two stationary pulsating fields 90 degrees apart in both time and space. Choosing a proper value of capacitor results in the stator currents being displaced by as much as 90 degrees in time producing the same kind of rotating field that can be produced in an ideal two-phase machine.

1.3 Induction Machine Model

The q-d model of a single-phase induction machine has been introduced in this section. The equivalent circuit of a single phase induction machine is shown in Figure 1.13 [4].

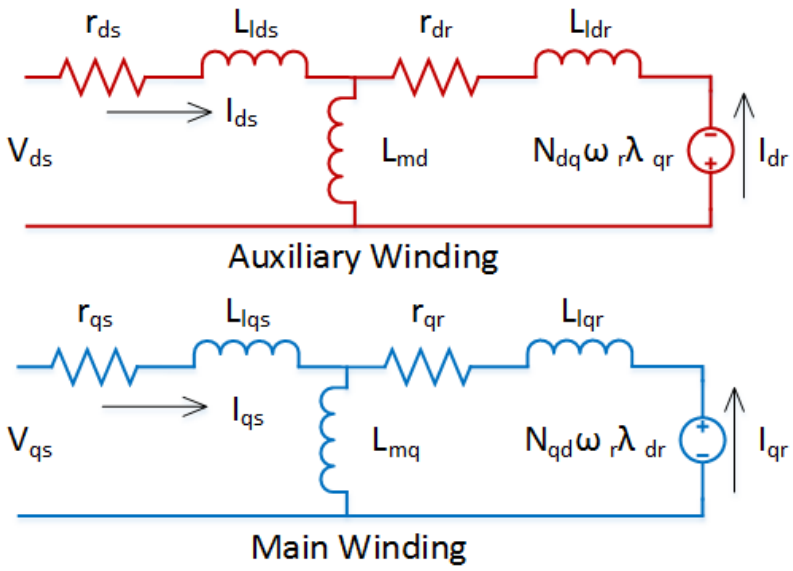

Figure 1.13: Equivalent circuit of a Single Phase Induction Machine

All parameters have been referred to the q stator winding in the above machine model. The q-d equations of the above model in the stationary reference frame are as follows:

$$p\lambda_{ds} = V_{ds} - r_{ds}I_{ds} \tag{1.1}$$

$$p\lambda_{qs} = V_{qs} - r_{qs}I_{qs} \tag{1.2}$$

$$p\lambda_{qr} = N_{qd}\omega_r\lambda_{dr} - r_{qr}I_{qr} \tag{1.3}$$

$$p\lambda_{dr} = -N_{dq}\omega_r\lambda_{qr} - r_{dr}I_{dr} \tag{1.4}$$

where, the q-d flux linkages are defined in terms of q-d currents as follows:

$$\lambda_{qs} = L_{qs} I_{qs} + L_{mq} I_{qr} \tag{1.5}$$

$$\lambda_{qr} = L_{qr} I_{qr} + L_{mq} I_{qs} \tag{1.6}$$

$$\lambda_{ds} = L_{ds} I_{ds} + L_{md} I_{dr} \tag{1.7}$$

$$\lambda_{dr} = L_{dr} I_{dr} + L_{md} I_{ds} \tag{1.8}$$

The Torque equation for the machine is as shown in the expression 1.9.

$$T = \frac{P}{2}\left(\frac{N_d}{N_q}\lambda_{qr} i_{dr} - \frac{N_q}{N_d}\lambda_{dr} i_{qr}\right) \tag{1.9}$$

1.4 Summary

The equivalent induction machine model discussed in Section 1.3 has been used to study, analyze and simulate the machine throughout this work. This model has also been used to determine the parameters of a single-phase induction machine under study which is described in detail in Chapter 2. Chapter 2 also discusses the most popular class of SPIMs i.e. capacitor-start SPIMs and how they can be used as two-phase motors.

Subsequently, in Chapter 3, this two-phase machine has been proposed to be used as a wind turbine generator coupled with power electronics. The work has been concluded in Chapter 4 along with suggestions for future work.

2 CAPACITOR START INDUCTION MOTOR AS A TWO-PHASE INDUCTION MOTOR

A majority of single-phase induction machines are capacitor-start motors. As discussed in Section 1.2.2, capacitor-start induction machines have two stator windings, namely the main winding and the auxiliary winding which are wound spatially 90° apart. In order to give a time shift of 90° in the excitation voltage, the auxiliary winding is connected to the main winding supply voltage by a *start* capacitor in series. Once the machine reaches about 80% of its rated speed, the mechanical switch disconnects the auxiliary winding from the AC supply. Since the auxiliary winding is used only to start the single-phase induction machine, and disconnected once the machine reaches a certain speed, these passive windings are made of poor quality wires in order to reduce machine cost, weight and size.

The premise explored in this chapter explores whether the poor quality auxiliary windings in the single-phase induction machine could be used actively for the complete machine operation without exceeding the rated operating temperature and loss conditions, and not effecting the machine's performance in terms of output, while reducing the power input. In order to study this, parameters of a typical single phase induction machine are determined which is discussed in Section 2.1. Consequently, steady-state analysis (Section 2.2) and dynamic simulation (Section 2.3) of the proposed configuration of the machine is performed to use the auxiliary winding actively. Finally, the description of the dynamometer setup built in order to experimentally verify the feasibility of using this proposed machine configuration is presented in Section 2.4.

2.1 Parameter determination of a Single-Phase Induction Machine

The nameplate details of a capacitor-start single phase induction machine which was chosen for the experiment is as shown in Table 2.1.

Table 2.1: Nameplate details of the selected Single phase Induction Machine

Century Electric			
CAT No.	C236	Part	B-158311-01
HP	1/3	Phase	1
Volts	115/230	Amps	5.2/2.6
RPM	1725	Insulation Class	A
Hz	50/60	AMB	40°C
Start Capacitor 163-193 MFD			

The next few sections discuss the parameter determination steps of the single phase machine in detail.

2.1.1 DC Resistance Test

First, the resistances of the main and auxiliary winding are measured by a DC current test based on Ohm's Law. Referring to Figure 1.13, the equivalent circuit of a single phase induction machine in case of DC excitation is as shown in Figure 2.1. Rated current is made to flow through the auxiliary and main windings in order to attain stator resistances which are equivalent to operating conditions' resistances. The ratio of the voltage imposed on the winding and the rated current gives the machine stator resistance.

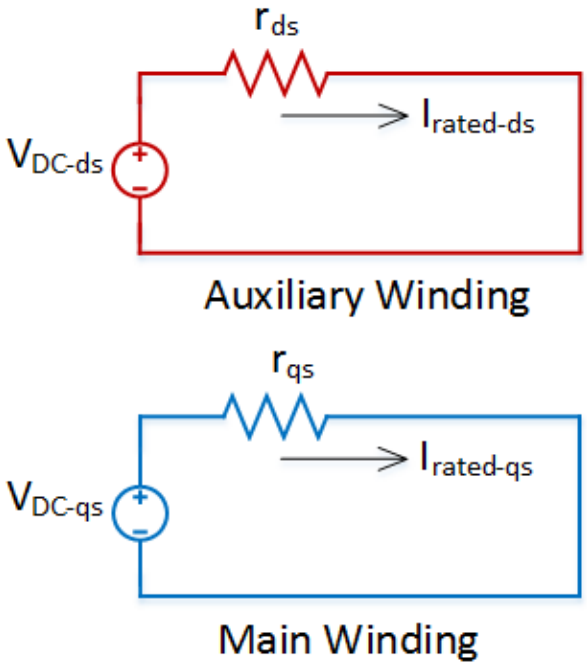

Figure 2.1: Equivalent circuit of a Single Phase Induction Machine during DC Resistance Test conditions

2.1.2 Blocked Rotor Test

Subsequent to a DC Resistance test, a blocked rotor test can be conducted on the two machine windings independently. A low voltage source is applied on only one of the windings at a time. Since a single-phase induction machine is not self-starting, the machine rotor will be blocked i.e. ω_r will be zero. In this scenario, the second winding will be completely inactive as can be observed in Figure 2.2. The excitation voltage is increased such that rated current flows through the winding.

Since the rotor winding branch will have a much lower impedance than the magnetizing branch, the current in magnetizing branch can be ignored. Hence, the active and reactive power input will give us the sum

of stator and rotor resistances and leakage inductances respectively. Since, stator resistances are already known, rotor resistances can be calculated.

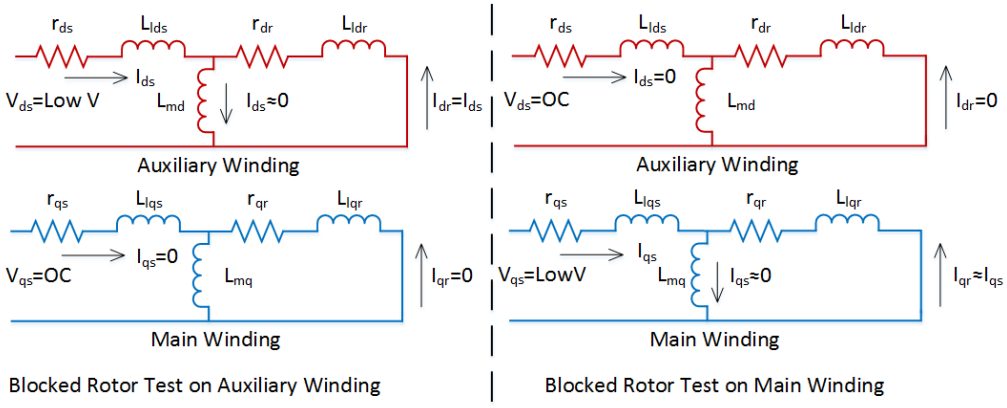

Figure 2.2: Equivalent circuit of a Single Phase Induction Machine during Blocked Rotor Test conditions

Similar test is conducted on the other winding. This test helps in the estimation of the rotor resistances and sum of leakage inductances of the two windings.

2.1.3 Turns Ratio Determination

The turns ratio is a significant parameter which can be defined as the ratio between the effective conductors in the auxiliary winding to the effective conductors in the main winding. The winding ratio was firstly determined by the technique discussed by Veinott [15].

The motor can be first run with the rated voltage V_q impressed on the main winding only and auxiliary winding voltage $V_{d'}$ can be measured. Subsequently, the motor can be run by applying voltage V_d across the auxiliary winding and then the main winding voltage $V_{q'}$ can be measured. Please note that the voltage across the auxiliary winding should be typically 18-20 % higher than the main winding voltage in order to run

the machine at the rated flux. The winding ratio can then be determined by the Expression 2.1.

$$N_{dq} = \sqrt{\frac{V_d V_{d'}}{V_q V_{q'}}} \tag{2.1}$$

Another way to determine this ratio is to simply take the square root of the ratio between the rotor resistances which can be derived from the equivalent circuit of the machine described by [4]. The rotor resistances can be determined by the techniques discussed in previous sections.

$$N_{dq} = \sqrt{\frac{r_{dr}}{r_{qr}}} \tag{2.2}$$

The results from the two expressions should conform with each other.

2.1.4 Determination of magnetizing and leakage inductances

The task of determining the q and d magnetizing inductances as well as the dividing the sum of leakage inductances between the stator and rotor leakages remain. Various techniques have been proposed in the literature [3, 11, 12] in order to determine these parameters.

However, a rather unconventional path has been taken in this study to determine the remaining parameters. A MATLAB code can be written in order to model the induction machine under study. With the determined machine resistances and the constraints of the sum of leakage inductances, the name plate parameters of the machine can be used. The additional constraint of ratios between the rotor leakage inductances and between the magnetizing inductances being a function of winding ratios can also incorporated into the code. The literature work [4, 7] on single phase induction machines gave a limit on the range of magnetizing inductances.

The code was tasked to determine the machine parameters such that the resulting machine design conform with the nameplate rating i.e. a rated operation of 1/3rd HP at 1725 RPM with input Q axis current of 5.2 A at 115V Q-Winding voltage.

2.1.5 Parameters of the Single Phase Machine

The parameters of a capacitor-start single phase induction machine using the above techniques was determined as shown in Table 2.2.

Table 2.2: Parameters of a Single phase Induction Machine

1/3 HP 115 Volt 60 Hz 4 Pole Motor			
Main Winding	r_{qs}=1.2	x_{mq} = 42.46	r_{qr} = 2.4
	x_{lqs}=3.74		x_{lqr}=2.17
Auxiliary Winding	r_{ds}=7.5	x_{md} = 59.12	r_{dr}=3.02
	x_{lds}=7.97	N_d/N_q=1.18	x_{ldr}=4.09

These machine parameters have been used for the analysis of using the single phase induction machine for further study.

2.2 Steady-state simulation of the proposed two-phase machine

The machine parameters determined in Section 2.1 were used to simulate the steady-state characteristics of the machine for the default configuration for which the machine is designed for. In this configuration, the machine when excited by a voltage source, is connected as a two phase machine with a start capacitor feeding the auxiliary winding as shown in Figure 2.3. Once the machine reaches about 80% of the rated speed (1500 RPM in this example), the mechanical switch disconnects the auxiliary winding, and the machine reaches its steady state load conditions.

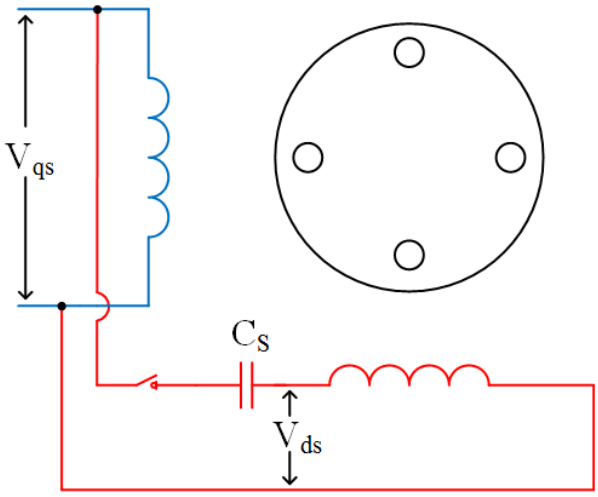

Figure 2.3: Capacitor Start Induction Machine Configuration

Figure 2.4 shows the per-unitized plots of the machine. In all the figures, it can be seen that the machine follows the red curve until its speed reaches 1500 RPM after which the switch disconnects the auxiliary winding, following the blue curve. Henceforth, the torque as well as the power output reduces as the machine is now using only a single winding for its operation. The efficiency of the machine increases as a result of zero current in the poor quality auxiliary winding.

The machine was now simulated for the capacitor-start capacitor-run operation as shown in Figure 2.5. The machine is connected to both the capacitors C_S and C_R until it reaches 80% of its rated speed after which the mechanical switch disconnects. However, it can be noted that in this configuration, the auxiliary winding is always connected to the excitation voltage by the run-capacitor C_R. Hence, the machine enters two-phase motoring operation.

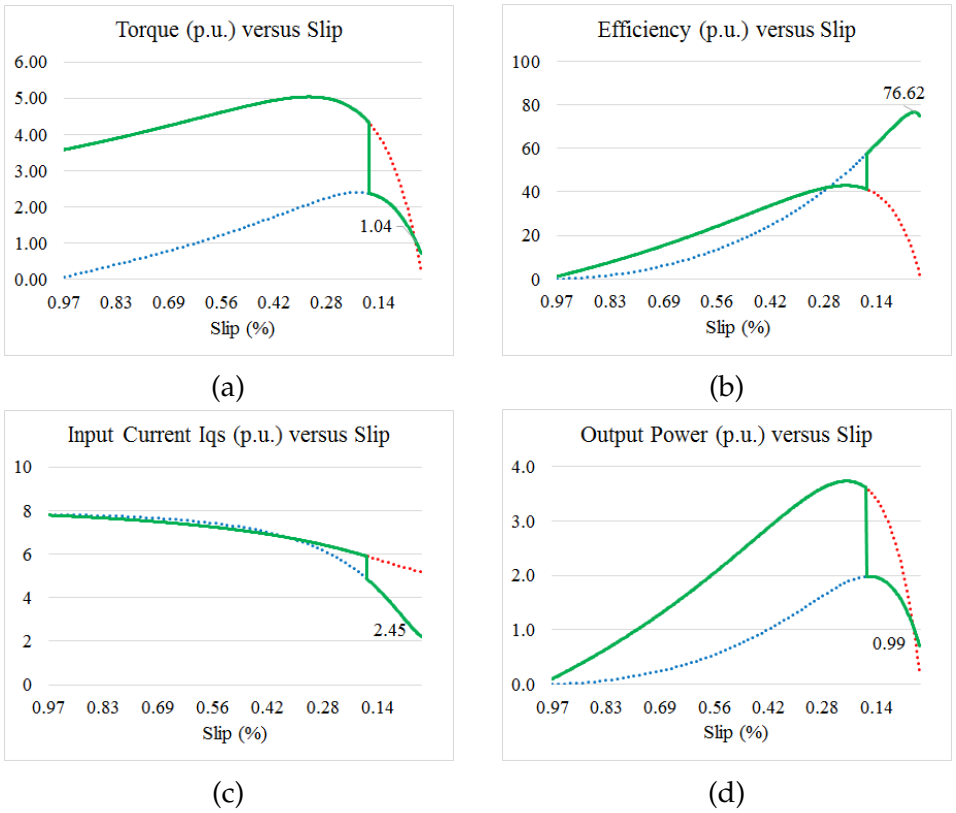

Figure 2.4: Steady-state plots for the CSIM Configuration of the machine

This configuration of the machine is used in two-value induction machines. However, in order to test whether an existing capacitor-start machine can be connected as a two-value induction machine, without hampering its rated performance, the test machine's parameters were simulated by connecting a run capacitor of $C_R = 20\mu F$.

Figure 2.6 shows some of the characteristics of the machine under test for this configuration. The effect of the value of the run capacitor C_R shall be discussed later. However, the case shown below is a general case for this machine under test. The current in the main winding reduces as compared to the rated configuration. The auxiliary winding now carries some current during the machine operation. It can be seen that there is an

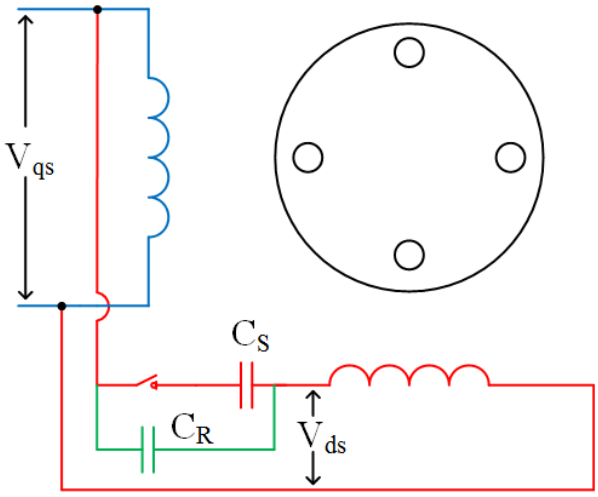

Figure 2.5: Capacitor Start Induction Machine Configuration

overall reduction in the total losses in the operating region of the machine with the distribution of currents between the main and auxiliary winding. The machine will hence run cooler if a run capacitor is added to run the auxiliary winding actively.

The machine gives higher power output and machine torque as can be seen from the bottom traces. This can be expected from the fact that now the machine is a two winding machine, carrying more flux. The efficiency of the machine increases by as much as 11% while the losses in the machine reduce by about 0.1 p.u.

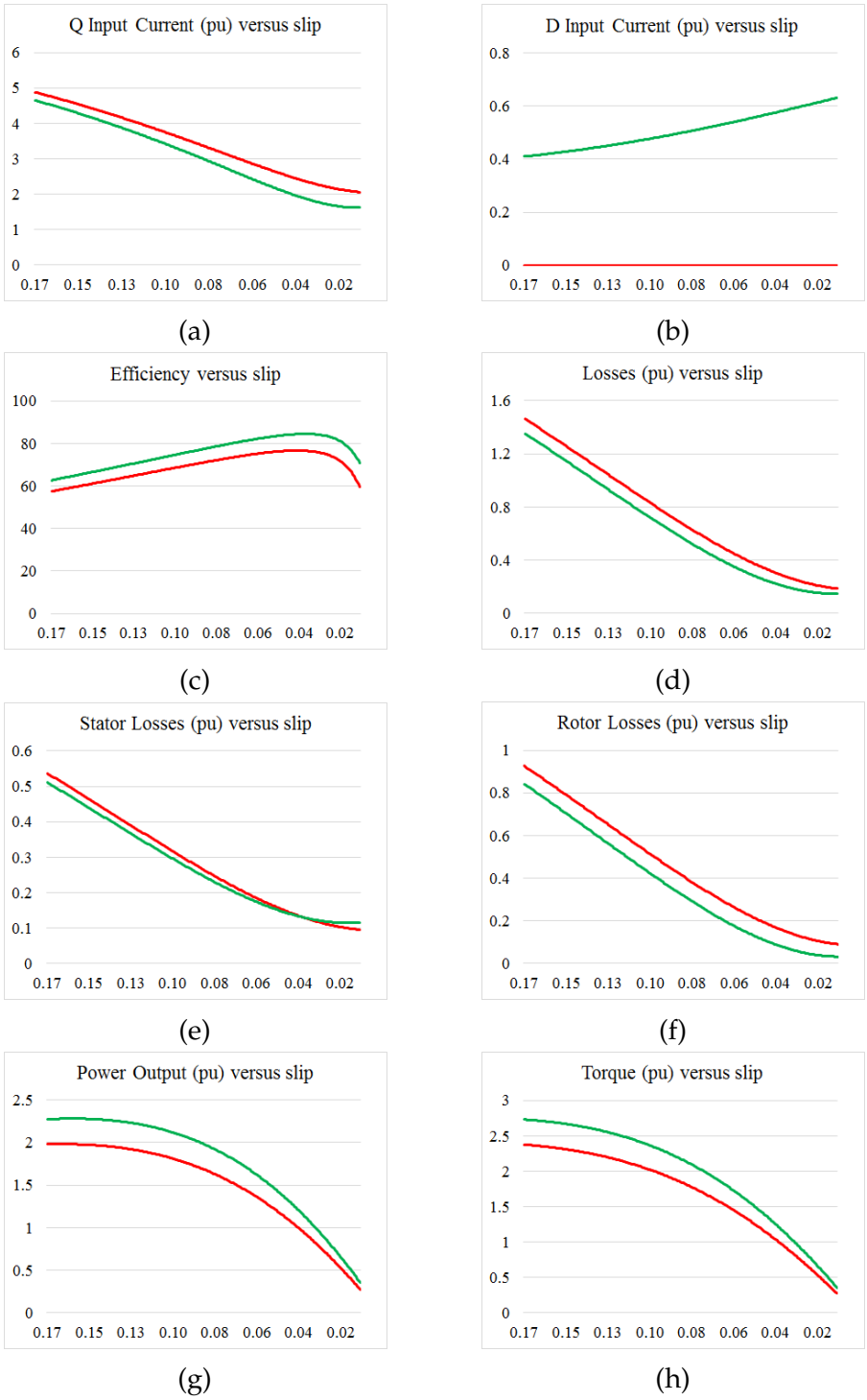

Figure 2.6: Steady-state plots for the CS-CR IM Configuration of the machine with run capacitor of 20 micro farads

It can be seen that the auxiliary winding stator resistance is as much as thrice the main winding stator resistance. If the value of the run capacitor is increased by a larger amount, the current in the auxiliary winding might increase in greater proportion as compared to reduction in losses in main winding. Hence, the run capacitor has to be chosen cautiously. The capacitor-start capacitor-run machine configuration was simulated for run capacitors varying from 10μF to 40μF. Figure 2.7 shows the results for this simulation exercise.

It can be seen that as the capacitor size increases, the current in the main winding reduces while the current in the auxiliary winding increases. This is because of the reduction in the run-capacitor impedance. However, since the auxiliary winding is made of poor quality, we can see that this leads to an increase in the stator losses. Not surprisingly, reduction in the q axis stator current leads to a reduction in the q axis rotor current. Similarly, reduction in the d axis stator current leads to a reduction in d axis rotor current. Since, there is not a very big difference in the q and d axis rotor resistances, it can be seen that there is an overall reduction in the rotor losses as well as the total losses in the machine. Hence, the machine can run at a temperature lower than the rated temperature, for run capacitors of value 10μF, 20μF and 30μF for most slip conditions, and 40μF for high slip operating regions.

Also, the machine can provide a more symmetrical and stronger rotating magnetic field with high value capacitors. Hence, it can be observed from the lower traces of Figure 2.7 that bigger run capacitors provide higher torque and power output.

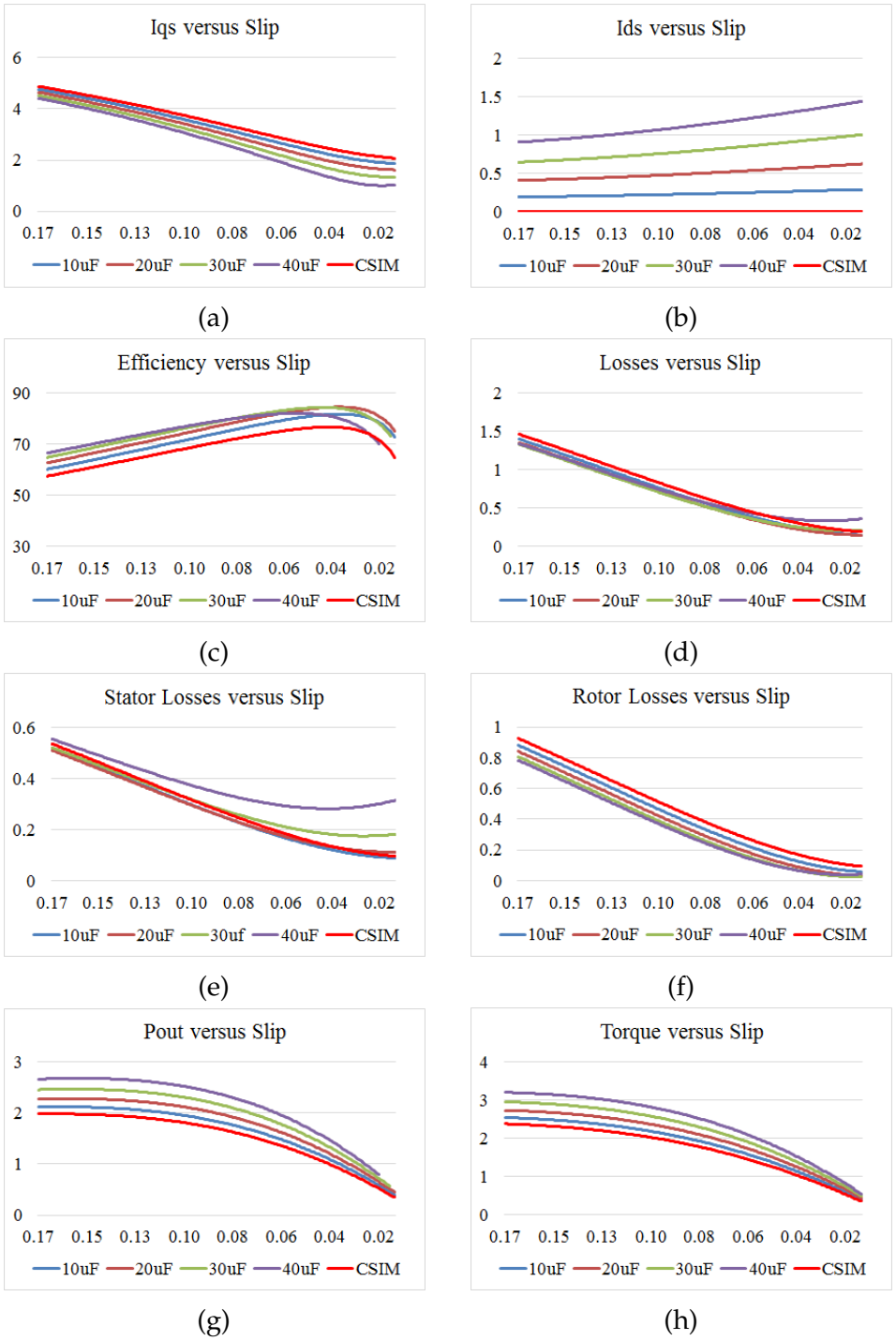

Figure 2.7: Steady-state plots for the CS-CR IM Configuration of the machine with varying run capacitors

Figure 2.8 gives an illustration of the performance improvement of retrofitting a run capacitor to a capacitor-start machine. If a capacitor in the range of 10μF is chosen, it can lead to an increase in the power output of as much as 0.142 p.u. and increase in machine efficiency of as much as 8% in low slip operating region. If a capacitor in the range of 30μF is chosen, it can lead to an increase in the power output of as much as 0.5 p.u. and increase in machine efficiency of as much as 8%.

It can hence be concluded from these steady-state machine simulation results that retrofitting a run capacitor to a capacitor start machine can help in increasing the performance of the machine in terms of its efficiency and power output. Additionally, due to loss reduction, the machine will run cooler increasing its lifespan.

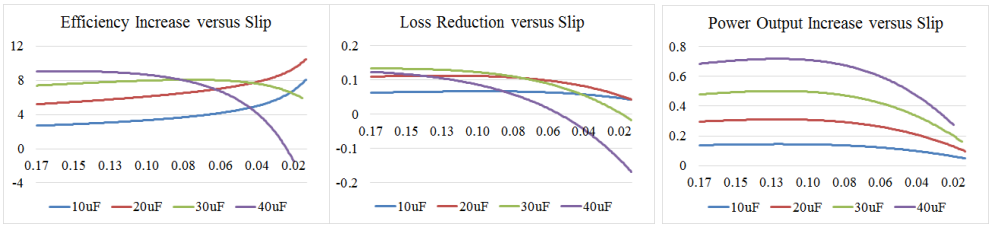

(a) (b) (c)

Figure 2.8: Difference between CSIM and CS-CR IM Operation

2.3 Dynamic simulation of the proposed two-phase machine

The dynamic simulation of the machine was done for the case when a single phase induction machine is line started.

The machine was first simulated for its rated default configuration. In this case, the machine is started as a two phase machine with a start capacitor of 180μF in series with the auxiliary winding. Once the machine reaches about 1500 RPM, the mechanical switch disconnects the auxiliary

winding and the machine reaches its rated load conditions. Figure 2.9a shows the simulation results.

The blue traces of Figure 2.9a shows the time during which the start capacitor is active while the red traces shows the machine operation when only the main winding is active. Once, the machine reaches an electrical speed of about 314 rad/seconds, the D axis stator current goes to zero. The machine finally reaches its rated Torque Conditions.

In the second case, the machine was simulated for the case when the machine is started with both start capacitor and run capacitor in parallel with each other. Once the machine reaches an electrical speed of about 314 rad/second, the start capacitor is disconnected with the run capacitor still in series with the auxiliary winding keeping the auxiliary winding active. Figure 2.9b shows the simulation results.

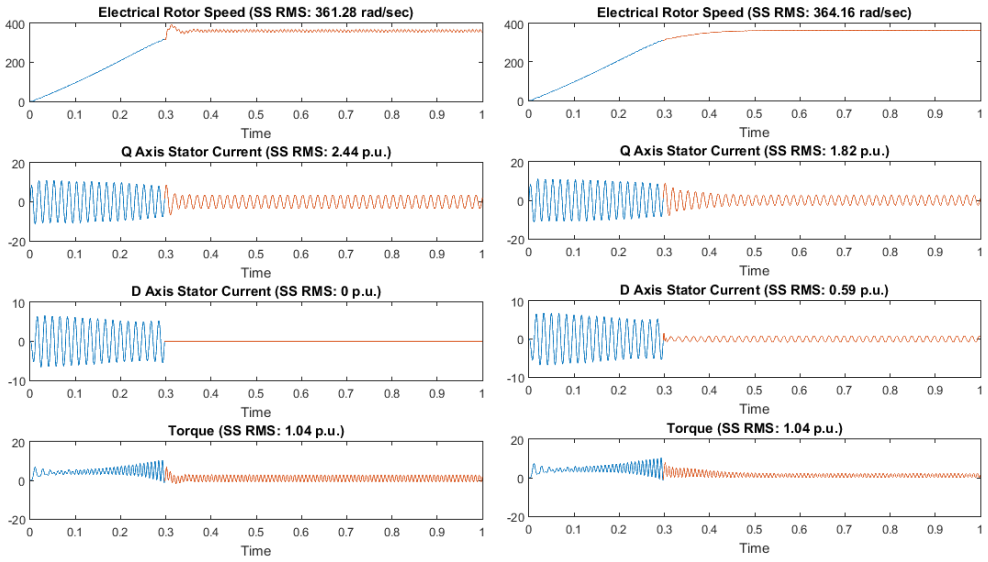

(a) Line start dynamic simulation curves of CSIM

(b) Line start dynamic simulation curves of CS-CR IM

Figure 2.9: Line start dynamic simulation of Induction Machine

It can be seen that the d axis stator carries a steady-state current of

0.59 p.u. while the current in Q axis stator reduces to 1.84 p.u. from 2.44 p.u. The load torque was kept the same in the two cases which is 1.04 p.u. However, it can be seen that the machine rated electrical speed increases from 361.28 rad/second to 364.16 rad/second indicating an increase in power output. Not surprisingly, the torque ripple is about 70% lesser in the case of an active auxiliary winding as compared to a passive case.

Figure 2.10 shows the plot of varying rotor flux along the two axis once the above machine configurations are line started. The blue traces shows the scenario when the start connector is still connected while the red traces shows the case when the start capacitor has been disconnected. The flux in the second case is higher as well as more circular indicating the uniformity of the rotor flux along the Q and D axis. It can be observed that the d-axis flux increases making the rotor flux more symmetrical.

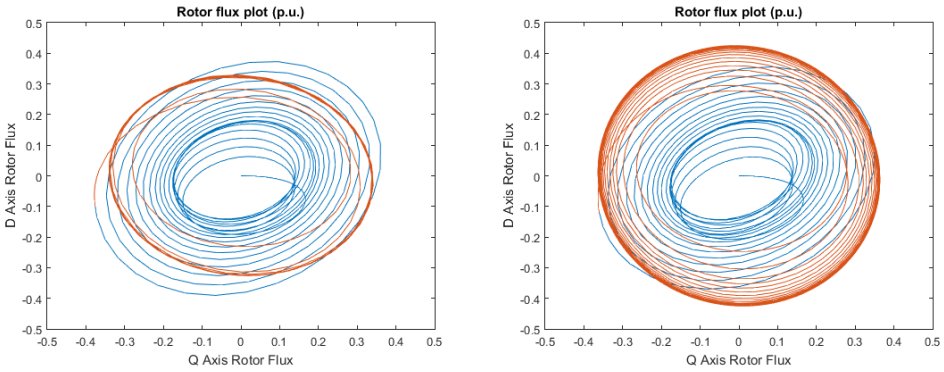

(a) Rotor flux plot of CSIM Configuration

(b) Rotor flux plot of CS-CR IM Configuration

Figure 2.10: Rotor flux plot of Single Phase Induction Machine

2.4 Experimental verification

A laboratory setup of the dynamo using the same machine under test was completed in order to verify the above simulation results. Figure 2.11

shows the dynamo setup. The induction machine under test was coupled with a DC Shunt Machine. This DC shunt machine was run as a separately excited DC Generator. Hence, the field windings of this DC motor was separately excited using a DC source.

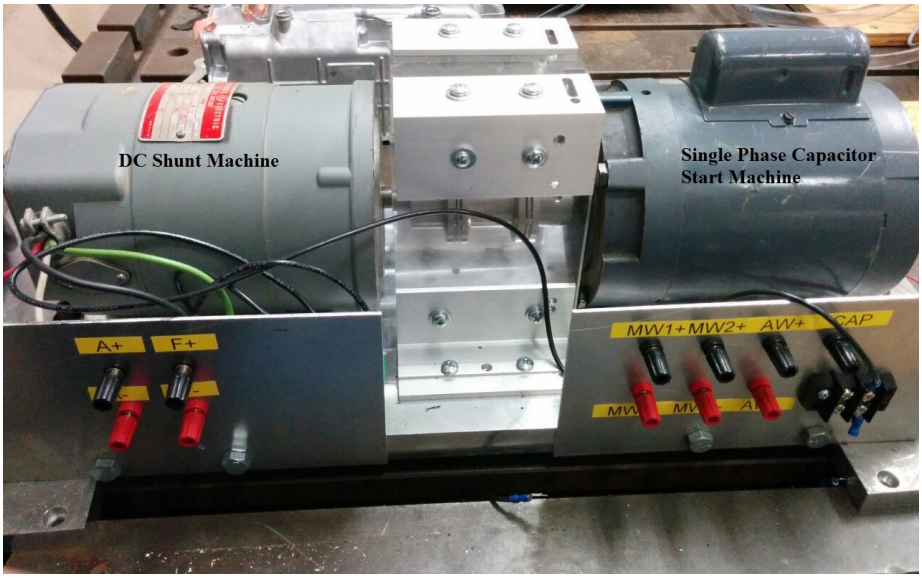

Figure 2.11: Laboratory Setup of the Dynamo

The nameplate details of the DC Shunt motor are shown in Table 2.3.

Table 2.3: Nameplate details of the DC-Shunt Machine

General Electric			
Model No.	5BCD56CD247	RPM	1725
HP	1/4	Volts	90A / 100F
Amps	2.75A / 0.45F	Insulation Class	F

Figure 2.12 shows the coupled circuit diagram of the two machines.

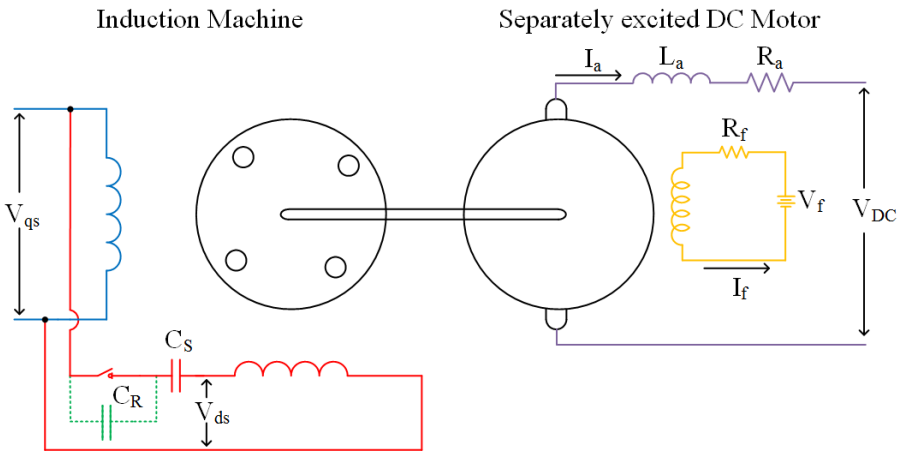

Figure 2.12: Coupled circuit diagram of the coupled machines

2.4.1 Mathematical Model

The mathematical model for a single-phase induction machine has already been presented in Section 1.3. This section deals with the mathematical model of a separately excited DC Machine which will simplify the analysis of the experimental results presented in this chapter.

Figure 2.13 shows the circuit schematic of a DC Machine. The field circuit equation is governed by expression 2.3 while the armature circuit equation is governed by expression 2.4.

$$V_f = I_f R_f \tag{2.3}$$

$$E_a - V_{DC} = R_a I_a + p L_a I_a \tag{2.4}$$

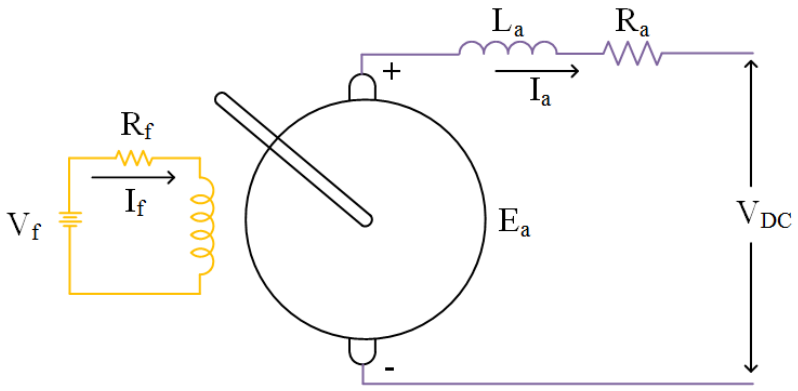

Figure 2.13: circuit diagram of a doubly fed DC Generator

The field circuit links the armature circuit which can be expressed by equation 2.5.

$$E_a = KI_f \tag{2.5}$$

where, the machine constant, K can be expressed as (during steady state conditions):

$$K = \frac{E_a}{I_f} = \frac{V_{DC} + R_a I_a}{I_f} \tag{2.6}$$

$$V_{DC} = R_{load} I_a \tag{2.7}$$

$$K = \frac{R_{load} + R_a}{I_f} I_a \tag{2.8}$$

The generated power can be given as follows:

$$T\omega_r = E_a I_a = KI_f I_a \tag{2.9}$$

This mathematical model along with experimental measurements have been used to calculate the operating efficiency and loss conditions of the single-phase induction machine.

2.4.2 Experimental Results

The dynamo was run at $115V_{DC}$ with the DC Shunt machine loaded with a resistive load (R_O) of 19.5 Ω. The operating conditions were varied by changing the field voltage V_f from 25V to 50V DC. By using equations 2.3-2.5, the calculation of the machine efficiency and other parameters could be completed. Table A.1 shows the measured and calculated data. Figure 2.14 shows the plots indicating efficiency improvement, loss reduction and power output changes.

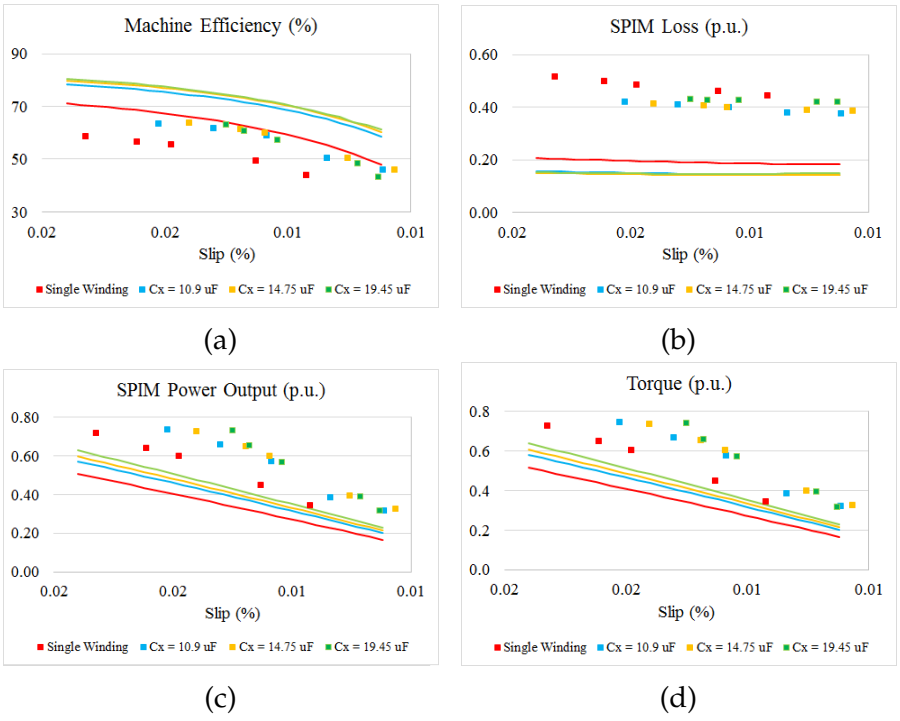

Figure 2.14: Plot of Efficiency improvement data from experiment. Solid lines indicate simulation results. Data points indicate experimental results

The x-axis of the plots in Figure 2.14 indicate the changing slip with changing field voltage, showing different operating conditions. The solid

lines in these plots indicate simulation results while the data points indicate the experimentally collected data.

It can be seen from Figure 2.14a that an efficiency increase of up-to 9% could be achieved by using the capacitor-start capacitor-run mode of operation by using a run-capacitor of about 10.9μF. The machine ran cooler, with reduction in machine losses of up-to 15W with the induction machine delivering higher power output. The simulation results indicated efficiency improvement of up-to 8% in this region.

It can be observed that with increasing value of run capacitances, the machine power output increases. However, the losses in the machine also increase due to increasing current in the poor quality auxiliary winding leading to a slight reduction in machine efficiency. The theoretical analysis of the effect of varying the run capacitor conforms with the experimental results.

It can be observed from Figure 2.14a and Figure 2.14b that the experimental machine efficiency is lower and machine losses are higher than the theoretical results. The difference between the simulation and experimental data is most probably a result of the approximation of ignoring machine core losses while determining the machine parameters. The experimental power output (Figure 2.14c) and torque output (Figure 2.14d) is higher than the theoretical predictions which can be attributed to certain inaccuracies in machine parameter determination.

2.5 Summary

Steady-state and dynamic simulation and experimental results verify that a capacitor-start single-phase induction machine can be used as a two-phase motor with improved efficiency and reduced torque ripple by retrofitting a run-capacitor. The next chapter deals with using this two-phase machine as a wind-turbine generator coupled with a dc-link inverter system.

3 INDUCTION MOTOR AS A GENERATOR

Single phase induction machines are widely used (and hence readily available), cheap, rugged and appropriate for fractional horsepower applications. This leads to the second premise of this work, that a capacitor-start single phase induction machine can be used effectively as a generator for realizing low cost wind turbine power systems as explored further in this chapter.

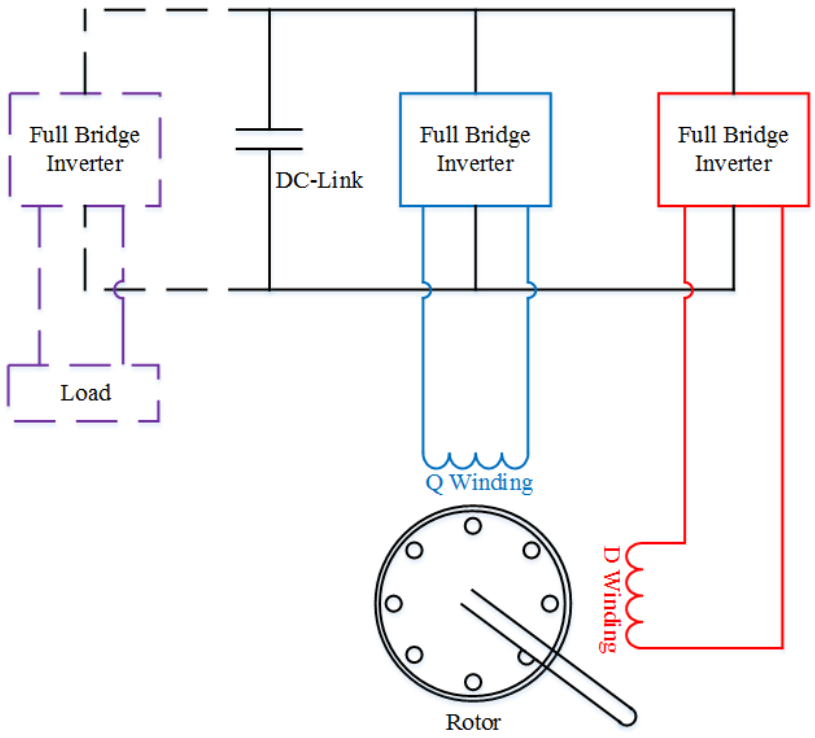

Figure 3.1: PWM Inverter-SPIM Generator System

The proposed single-phase induction generator scheme with a dc link PWM Inverter System is as shown in Figure 3.1. Two full-bridge DC to AC Inverters, fed from a dc link, are connected to the two windings of the single phase machine. The system can be loaded at the dc bus or an ac load

can be connected via another full-bridge inverter. When this system is used in a wind turbine generation system, the rotor is connected to a suitably sized turbine through a gear box or a belt drive. Hence, in this scenario, the two machine winding - inverter systems are always supplying power to the dc link. It is assumed that the two inverters may be controlled such that the magnitude and angle of the ac voltage at the winding terminals may be regulated independently at all frequencies, so as to track the rotor speed to facilitate appropriate extraction of wind power.

This design may been chosen in order to work with a wide range of rotor speeds and load conditions. It will be shown that using this configuration, the machine can operate at voltages within 1 p.u. and still give power more than 1 p.u. under general operating conditions, while the operation is constrained such that the machine losses are within the rated loss limits.

A brief review of wind power generation is developed in Section 3.1. The steady state operation of the SPIM as an inverter driven generator is developed in detail in 3.2. Matching between a suitably sized wind turbine and the induction generator to realize the appropriate operating speeds are discussed in 3.3. VA ratings of the inverters that may be used with the systems are discussed in 3.4.

3.1 Wind Power Extraction from Induction Generator

In a simplified and ideal case, wind will flow near the wind turbine as shown in Figure 3.2 [10].

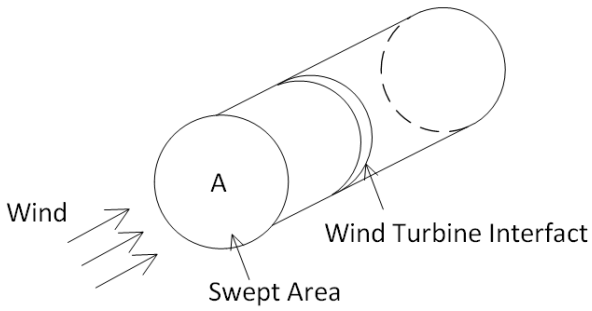

Figure 3.2: Idealized and Simplified Wind Behavior

Some percentage of the kinetic energy contained in the volume of the wind which hits the turbine blades is transferred to the wind turbine. The kinetic energy of the air-stream is based on the density of air ρ and its velocity w. Consequently, the power of this air crossing the surface A, can be calculated which can be given by the Expression 3.1.

$$P_{wind} = \frac{1}{2}\rho A w^3 \tag{3.1}$$

If, at this surface A, 100% of the power can be extracted from the wind, all of the kinetic energy of the air would be removed and the air would stop moving completely. Over this surface, air molecules would enter but none would escape, thus causing a collection of molecules and a violation of the given constraints. Conversely, if the air molecules were not slowed at all, no power would be extracted. Somewhere, then, between 0 and 100%, lies the maximum amount of power that can be extracted from a quantity of wind which can be incorporated in Expression 3.1 in order to obtain the available wind power Expression 3.2.

$$P_{wind-available} = c_P \frac{1}{2}\rho A w^3 \tag{3.2}$$

An upper bound for this factor was determined by Albert Betz in 1926 using the simplified model given in Figure 3.2 to be 59% [2]. In typical turbines, the coefficient of performance factor c_P is lower (as discussed in later sections). Also, in most cases, the air density may be assumed to be a constant value of ρ is 1.225 kg/m^3.

Hence, it can be seen that the power contained in the air increases by a factor of cube with increase in the wind velocity (Equation 3.2). It is worth noting that the induction machine typically follows a linear pattern of power rise with increasing rotor speed as shown in Figure 3.3. Two different machine traces have been shown in the Figure marked by red trace and blue trace. It can be observed that over a certain region of wind turbine operation (marked by circles in Figure 3.3), the machine will be over-rated. Not surprisingly, when the wind speed increases, the power increases much faster in a cubic fashion leading to the machine being under-rated for high wind speed operating regions.

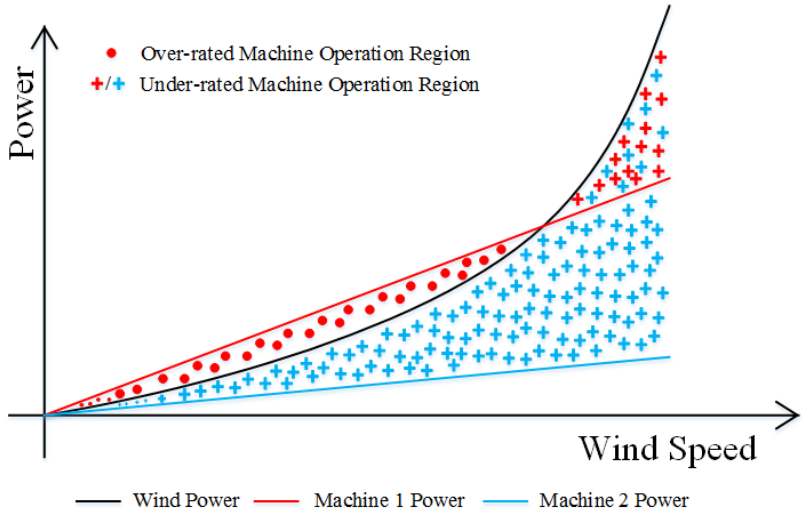

Figure 3.3: Wind Power utilization pattern of an Induction Machine

3.2 Induction Generator Operation

The steady state analysis of SPIMs for the proposed wind-turbine power generating system is developed further in this section.

3.2.1 Constant Excitation Frequency Operation

As an initial case-study, the machine operation when the excitation frequency was kept constant at 60 Hz. The rotor speed was varied beyond the synchronous speed till about 10 % slip or 2000 RPM. The machine operating conditions were optimized such that the stator and rotor losses stay below the rated values of 0.13 p.u. and 0.17 p.u. with the machine providing maximum possible power output. The magnitude and phase angle of the currents and voltages in the stator windings are determined under these conditions. Figure 3.4 shows the required excitation conditions of the two machine windings with varying rotor speed.

The voltages and currents in this chapter are per-unitized with the voltage and current being the base units unlike the previous two chapters (where voltage and power were chosen as base units). Hence, 1 p.u. voltage and 1 p.u. current is equivalent to 115V and 5.2A respectively.

It can be observed that with increasing rotor speed, the winding voltages have to be reduced in order to limit the machine losses. The Q current shows a rising trend and starts reducing as a rotor speed increases in order to limit losses. The Q-D currents form an angle of greater than 90° with their respective voltages indicating the power output from the two machine windings. Not surprisingly, the angle between the Q and D voltages have to be maintained to about 90° in order to get the maximized power output from the machine.

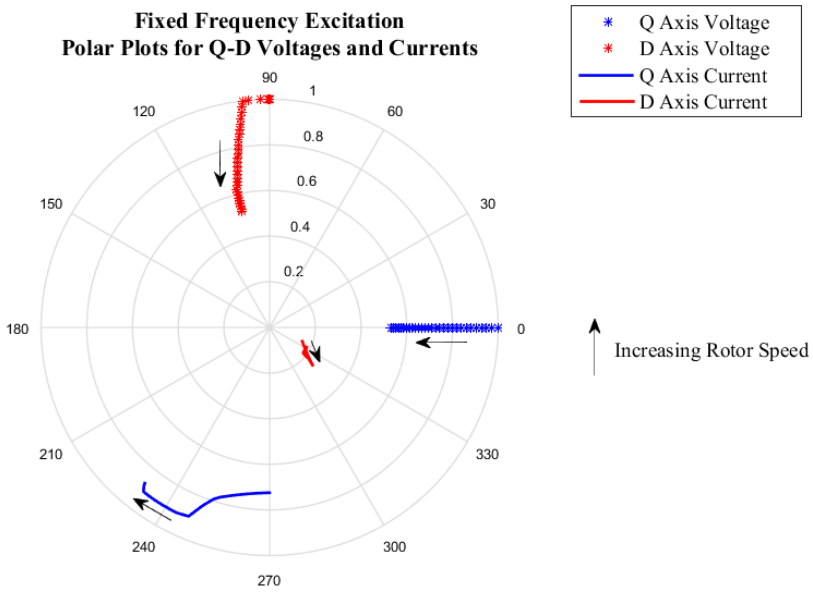

Figure 3.4: Polar Plot of Voltages and Currents in case of fixed excitation frequency

Figure 3.5 shows the machine power output and efficiency plots. It can be observed that the machine shows the typical induction machine power output pattern of generating mode wherein the power increases, reaching a peak, subsequent to which the power output starts to fall (Figure 3.5a). The same trend can be observed in the efficiency plot (Figure 3.5b).

(a) (b)

Figure 3.5: Power and Efficiency plots in case of fixed excitation

It can be observed that the power trace shows a linear trend until the rotor speed reaches about 1900 RPM after which the power output falls linearly. As may be observed in Figure 3.3, significant amount of wind power is lost above the rotor speed of 1900 RPM. The rotor speed operating range wherein the machine power is rising is only from about 1800 RPM to 1900 RPM subsequent to which the wind turbine has to be yawed so as to limit the power input and rotor speed of the machine. The peak power output from the machine in this case is 1.23 p.u. or 304W with the machine efficiency of 82.2 %.

3.2.2 Variable Excitation Frequency Operation

As it is concluded that in constant frequency operation of the SPIM, the wind power can only be extracted in limited wind speed ranges i.e. only above 1800 RPM. However, in order to deduce power from low wind speed operations, the excitation frequency of the machine can be reduced. This allows the machine to operate as a generator even at low rotor speeds. Variable excitation frequency operation optimization is performed on the case-study machine in order to determine the optimum excitation conditions of the machine for rated machine losses. Figure 3.6 shows the results obtained from this optimization study.

It may be observed that there is a near linear increase of excitation voltage as the rotor speed increases from 450 RPM (cut in speed) to 1900 RPM (maximum speed). The currents in the windings are at their rated amplitude at nearly every excitation frequency in order to give maximized power output within the loss limits. However, it can be observed that since the current remains nearly constant, this leads to constant flux operation at various stator frequencies. Hence, in order to maintain maximized output, the voltage rises linearly with the stator frequency until nearly 60 Hz (constant V/Hz operation).

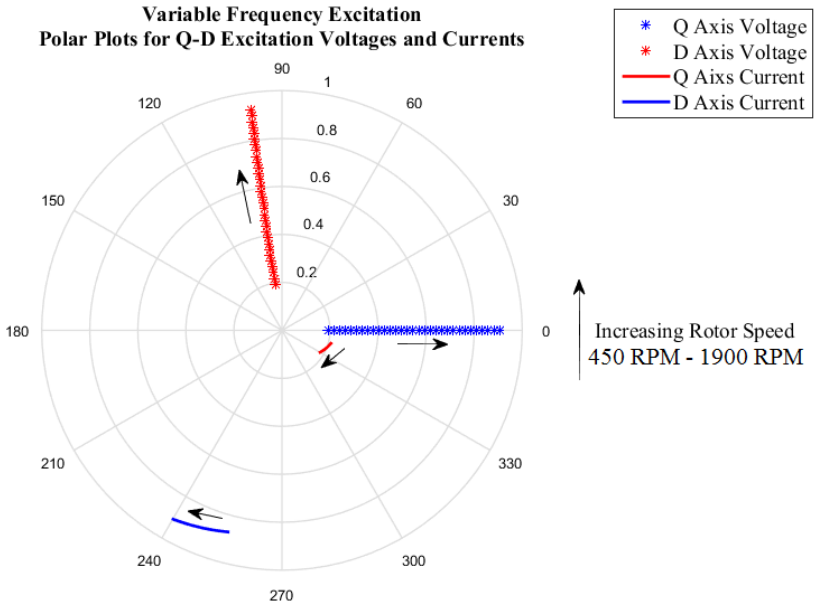

Figure 3.6: Polar Plot of voltages and currents in case of variable excitation frequency

The trend continues beyond this frequency range. However, since higher excitation frequency will lead to higher core losses, operation beyond base speed would be precluded. These conditions lead to nearly constant torque operation below the base speed.

It is interesting to observe that the Q and D currents are at exact 90° in order to maintain maximum power output. The voltages stay at nearly 98-99°. It can also be observed that the voltages fall short of 1 p.u. and reach a maximum of 0.92 p.u. at 60 Hz operation.

Figure 3.7 shows the power and efficiency of this operation. As can be expected in a constant V/Hz operation, the input and output power rise in a linear fashion which can be seen in Figure 3.7a. The losses are maintained at their peak value. However, with increasing voltage / excitation frequency, the power output increases. This leads to higher efficiency

operation at higher stator frequencies. Figure 3.7c shows the corresponding linearly increasing excitation frequency with increasing rotor speed. Figure 3.7d shows the total active and reactive power output delivered from the machine to the inverter system.

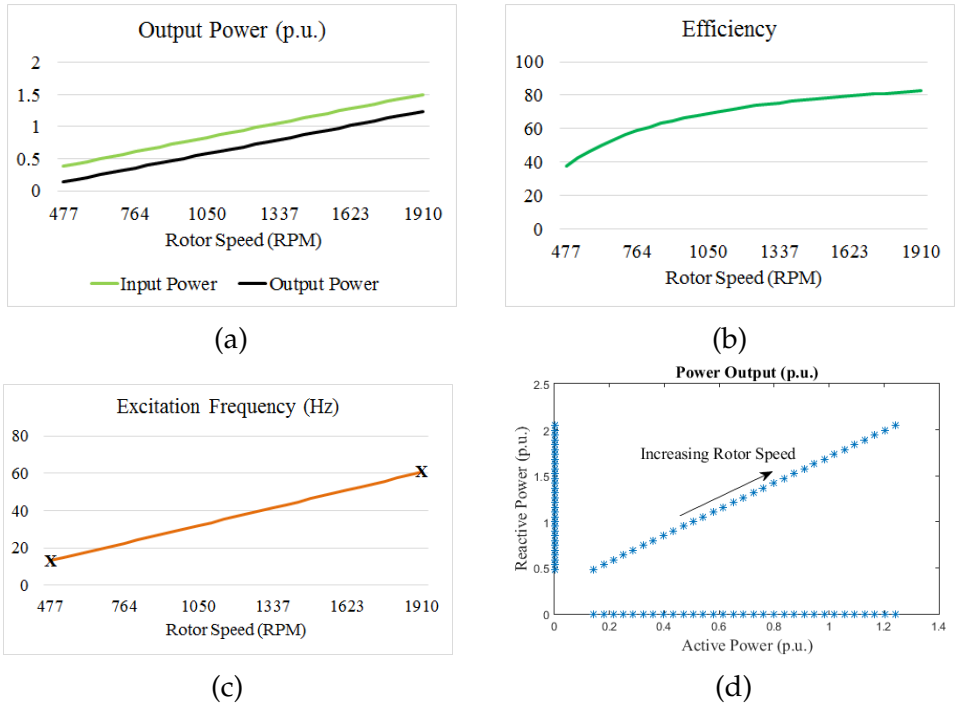

Figure 3.7: Power and Efficiency plots in case of variable excitation

The maximum theoretical output that can be obtained in this operation is 1.24 p.u. or 308W with an efficiency of 82.5%. This is comparable to the fixed frequency operation. However, it can be observed that the range of frequencies over which this operation can be extended is increased from the relatively small window of 1800 RPM-1910 RPM to large window of 450 RPM-1910 RPM, thus increasing the overall energy harvest from the turbine, particularly at low wind conditions.

3.2.3 Dynamic Simulation

The dynamic simulation of the discussed topology was done in MATLAB environment. Figure 3.8 shows the results for two cases (shown in Figure 3.7c). In the first case (Figure 3.8a), the rotor speed was maintained constant at 1909 RPM. At time zero, the Q and D winding voltages were applied at the excitation frequency of 60.6 Hz. It was be observed from the red and blue voltage traces that the D winding voltage leads the Q winding voltage by about 98°. The starting behavior of the currents and power output can be observed from the bottom three plots. The machine electrical power can be seen to be negative indicating the generating mode of operation of the machine.

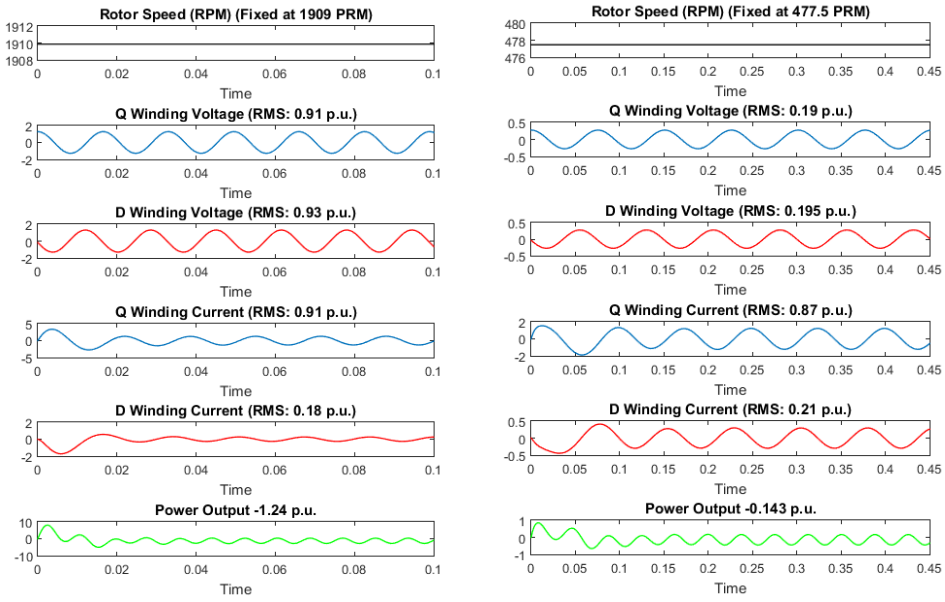

(a) Excitation Frequency of 60.60 Hz (b) Excitation Frequency of 13.25 Hz

Figure 3.8: Dynamic Simulation plots in case of variable excitation

Similar analysis was done for the case of low rotor speed operation wherein ω_r = 477.5 RPM. The low excitation frequency of 13.25 Hz can

be observed from the excitation voltages. Since the machine is operating at low prime-mover power, the electrical power output from the machine is only 0.143 p.u. However, the currents are very near to their maximum allowed values in order to have rated machine losses.

It can be seen from Figure 3.8 that the dynamic simulation results conform with the steady-state analysis for this generating operation.

3.3 Wind Turbine Design

Typical small wind turbines of fractional horsepower ratings are carved in wood, belonging to a family of wind turbines designed by Hugh Piggott [8]. The main design goals of these turbines are economical viability, ruggedness, ease of construction and good performance at low to medium wind speeds (3 to 10 m/s). This line of turbines, range in diameter from 1.2m to 4.2m.

The coefficient of performance factor, c_p, introduced in Section 3.1, is generally a function of the tip speed ratio λ, which depends on the turbine rotor speed and the particular wind velocity. Tip speed ratio, λ is defined as the ratio between the tangential speed of the tip of a blade and the actual velocity of the wind, w.

$$\lambda = \frac{\omega_b R}{w} \tag{3.3}$$

where, ω_b is the speed of the blade in rad/s and R is the radius of the wind turbine. The relationship between c_p and λ is rather complex, depends on various geometric features of the turbine blades and air stream properties.

Wind tunnel data on the performance of Hugh Piggott's 1.2m diameter rotor has been collected by Monteiro et al. [6] to characterize this relationship. This performance data determines various tip speed ratios and

the maximum possible coefficient of performance for the wind turbine at different wind speeds. This performance data has been used in this work to integrate the design of the proposed induction generator system with Hugh Piggott's wind turbine design. Table 3.1 provides the details from this study.

Table 3.1: Performance data of Hugh Piggott's Wind Turbine design

Optimum operating conditions for Piggott 1.2m Wind Turbine		
Wind Speed (w)	Coeff. of Perf. ($c_{P_{max}}$)	Tip-Speed Ratio (λ_{max})
3 m/s	0.32	6.5
3.7 m/s	0.34	6
4.4 m/s	0.36	5.9
5.5 m/s	0.38	5.2
7.2 m/s	0.4	4.9
7.7 m/s	0.4	4.9

The availability of this data for a wind turbine design and wind speed conditions for the location where the wind turbine is to be installed is critical for choosing the speed ratio (g), wind turbine area and machine rating. It shall be assumed that the data presented in Table 3.1 can be extended to Piggott's other diameter designs.

If it is assumed that the maximum likelihood wind speed in a particular location where the wind turbine induction generator is to be installed is 7.2 m/s, the gear ratio (g) between the wind turbine diameter and machine rotor and wind turbine sweep area may be determined in order to obtain an optimum operating point. A Piggott turbine design with a diameter of 2.4m [5] and a speed ratio of 6.8 gives a power output of 410W for a rotor speed of 1910 RPM, with a tip speed ratio of 4.9. In this case, the induction machine will operate at a power input of 373W, hence utilizing most of the wind power available.

Once the sizing of the wind turbine is done at the optimum operating point, the power output at various other less likely wind speeds can be obtained. Figure 3.9 illustrates the variation of wind turbine developed power and the induction generator's power capability at various rotor speeds.

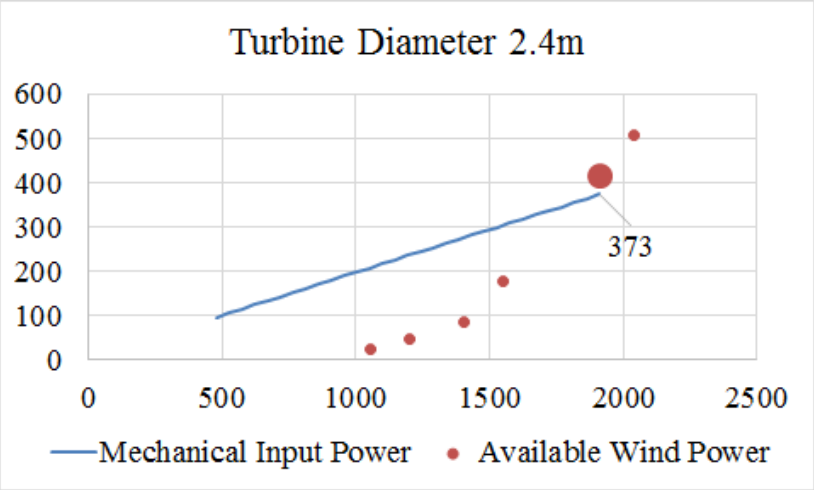

Figure 3.9: Available and extracted wind power from a 2.4m diameter wind turbine.

It can be observed that the machine is over-rated for lower wind speed operations if a diameter of 2.4m is chosen. Since, it has been assumed that the mostly likely wind speed is 7.2 m/s, the possibility of operating in the over-rated machine operating region is low. If the wind speed is higher, the wind turbine can be yawed in order to limit the machine rotor speed to 1910 RPM. When the wind speed is 7.2m/s the machine will operate at the optimal operating point, utilizing 91% of the available wind power. Similar design technique can be followed for other induction machines and wind turbine blades sizes in order to meet the local requirements of the wind-turbine generator system.

Please note that in case of fixed frequency operation, only limited wind energy can be harnessed. Variable frequency operation widely extends

the possible operating area for the machine.

3.4 VA Rating of the Inverters

The maximum power output at which the inverter fed SPIM generation system can be expected to operate is at 60Hz, beyond which the machine core losses would increase. It can be observed from Figure 3.6 that the voltages and currents reach a maximum of about 0.9 p.u. at this operating frequency. Table 3.2 shows the other operating conditions of the inverters.

Table 3.2: Voltage and current operating conditions at 60Hz

60Hz Operation of DC link Inverter SPIM Generation System				
	Q Winding		D Winding	
	Q-Voltage	Q-Current	D-Voltage	D-Current
p.u.	0.91	0.91	0.93	0.18
V/A	104.23V	4.72A	106.63V	0.96A
Combined VA Rating of Inverters: 0.99 p.u.				

It can be concluded that the inverters together have to be rated for only 1 p.u. for the two active single phase machine windings.

3.5 Summary

In this chapter, a dc-link PWM inverter single-phase induction machine system has been proposed. Detailed analysis and simulation results show that this system can be used as an inexpensive wind-turbine generator system. The same capacitor start single-phase induction motor introduced in Chapter 2 can be used as a generator having a theoretical efficiency improvement of 6% over its motoring operation. The two inverters coupled with the two windings of the SPIM together have to be rated to only 1 p.u.

It has been assumed that the two inverters can be controlled such that the magnitude and angle of the ac voltage at the two winding terminals may be regulated at all frequencies, so as to operate the machine at the maximum power output operating point.

4 CONCLUSION AND FUTURE WORK

Single-phase induction machines are widely used for domestic and agricultural applications in capacitor-start modes. In spite of their low operating efficiency of approximately 60-70%, these machines are prevalent in single-phase power supplied areas due to their high-torque capabilities and low costs as compared to other classes of single-phase machines.

This work aimed at accurately characterizing these machines and working towards improving their efficiency. Steady-state and dynamic modeling have been performed to investigate them. With the idea of using it as a two-phase machine, its auxiliary winding, which is used for starting, is actively utilized by adding a run-capacitor in parallel with the centrifugal switch. Using this configuration, the machine retains its high-starting torque capability. Moreover, the additional optimal capacitance helps maintain the total losses in the machine within the rated value by controlling the current in the two windings thereby improving the operating conditions of the machine. The machine has been tested in the laboratory for its parameters. Simulations and further laboratory tests indicate that the efficiency of CS-SPIM could be significantly improved by about 8-9%. Additional temperature rise tests on the winding indicated no untoward effect in the winding thermal loads.

Market investigations in California show an annual savings of approximately 75 million units of electricity (or $9 million) if a mere 2.5% of electricity consumed in water pumping, is used by CS-SPIM. Furthermore, this minor retrofitting to the machine can also be extended to household and other applications.

This two winding machine has been subsequently proposed to be used as a generator coupled with wind turbine and inverters for supplying dc and/or ac loads. Conventional wind turbine generators typically use permanent magnet machines which are often expensive and use rare earth

magnets. On the other hand, this work presents an inexpensive off-the shelf wind turbine generator system using the single-phase induction machine for fractional horsepower applications. Both the constant and variable excitation frequency operation proposed in this work offered a theoretical power output increase by about 24% with a theoretical efficiency of 82.5% in generating mode against 76% motoring mode efficiency. Thus,

The potential for future work in this area includes discovering areas and applications on the field where retrofitting a run-capacitor in capacitor-start induction machines is an added advantage in terms of efficiency improvement and torque ripple reduction.

The inverter system can be investigated for whether the three inverters (two Q/D Winding Inverters and one ac load inverter) could be replaced by a three or four legged inverter with a common neutral point. The implementation of the two proposed variable and fixed excitation frequency schemes in the laboratory prototype is also a work for future.

Appendix A EXPERIMENTAL RESULTS DATA OF THE DYNAMOMETER

The experimental results of the laboratory prototype built (please refer to Section 2.4.2 for details) in order to determine the efficiency improvement of a capacitor-start machine after retrofitting a run capacitor has been recorded in this section of the thesis.

Table A.1 records the measured power input to the single-phase induction machine and the power output from the separately exicted DC-Shunt Generator. The SPIM coupled DC-Shunt Machine rotor speed has been recorded using a stroboscope.

The recorded data along with the mathematical model of the two machines discussed in Section 1.3 and Section 2.4.1 have been used to calculate the single-phase induction machine output and losses which have also been provided in Table A.1. The results of this laboratory exercise have been discussed in Section 2.4.2.

Table A.1: Experimental Data recorded from the Dynamometer

Measured										Calculated		
I_{qs}	W_{qs}	V_{ds}	I_{ds}	W_{ds}	V_{DC}	V_f	ω_r	P_{in-IM}	P_{out-DC}	P_{out-IM}	Eff_{IM}	Eff_{DC}
Capacitor-start connection												
4.32	196.24	OC	0	0	37.39	25	186.56	196.24	71.69	86.13	43.89	83.24
4.42	225.60	OC	0	0	42.64	30	186.17	225.60	93.24	111.97	49.63	83.27
4.62	269.40	OC	0	0	49.29	40	185.52	269.40	124.59	149.66	55.55	83.25
4.67	283.20	OC	0	0	50.98	45	185.26	283.20	133.28	160.17	56.56	83.21
4.80	305.90	OC	0	0	53.91	50	184.87	305.90	149.04	179.14	58.56	83.20
I_{qs}	W_{qs}	V_{ds}	I_{ds}	W_{ds}	V_{DC}	V_f	ω_r	P_{in-IM}	P_{out-IM}	P_{out-DC}	Eff_{IM}	Eff_{DC}
Capacitor-start capacitor-run connection C_X = 10.90μF												
3.29	95.34	165.75	0.84	77.05	35.99	25.00	187.15	172.39	66.42	79.35	46.03	83.71
3.32	113.42	165.28	0.84	76.94	39.57	30.00	186.72	190.36	80.30	95.92	50.39	83.71
3.48	165.01	163.66	0.83	76.21	48.18	40.00	186.25	241.22	119.04	142.18	58.94	83.72
3.59	189.68	163.11	0.82	76.19	51.73	45.00	185.85	265.87	137.23	163.90	61.65	83.73
3.68	212.30	161.92	0.81	75.56	54.71	50.00	185.43	287.86	153.50	183.32	63.69	83.73
Capacitor-start capacitor-run connection C_X = 14.75μF												
2.93	66.97	172.76	1.17	109.95	36.40	25.00	187.24	176.92	67.95	81.21	45.90	83.66
2.95	85.82	172.12	1.16	109.45	40.12	30.00	186.87	195.27	82.54	98.66	50.52	83.67
3.11	140.78	169.85	1.14	107.73	49.34	40.00	186.24	248.51	124.84	149.17	60.03	83.69
3.15	153.39	170.44	1.14	108.67	51.32	45.00	186.06	262.06	135.06	161.40	61.59	83.68
3.24	175.46	169.60	1.14	108.10	54.33	50.00	185.66	283.56	151.37	180.88	63.79	83.69
Capacitor-start capacitor-run connection C_X = 19.45μF												
2.49	28.11	182.70	1.59	154.76	35.90	25.00	187.12	182.87	66.09	79.06	43.23	83.59
2.51	47.46	182.02	1.59	154.25	39.87	30.00	186.96	201.71	81.52	97.51	48.34	83.60
2.59	94.58	180.35	1.57	152.79	48.07	40.00	186.34	247.37	118.50	141.70	57.28	83.62
2.63	118.40	177.92	1.54	149.51	51.48	45.00	186.08	267.91	135.91	162.51	60.66	83.63
2.71	140.33	177.18	1.53	148.78	54.53	50.00	185.95	289.11	152.49	182.33	63.06	83.63

Appendix B EQUATION SOLVER CODE FOR SINGLE WINDING MACHINE

```
%%%%%%%%%%%%%%%%%%%%%%%%%%%%%%%%%%%%%%%%%%%%%%%%%%%%%%%%%%%%%%%%
% File Name: SinglePhaseOperation.m
%%%%%%%%%%%%%%%%%%%%%%%%%%%%%%%%%%%%%%%%%%%%%%%%%%%%%%%%%%%%%%%%
% This file constains the machine equations
% to solve for Single Winding Machine after
% the machine's auxiliary winding has been
% disconnected
%%%%%%%%%%%%%%%%%%%%%%%%%%%%%%%%%%%%%%%%%%%%%%%%%%%%%%%%%%%%%%%%

clear all;
clc;

% Machine Voltage condition
Vqss1 = sqrt(2)*115;
Vqss2 = 0;

% Excitation Frequency
we = 377;

% Machine Resistances
rqs = 1.2;
rqr = 2.4;

% Machine Inductances
Llqs = (3.74)/(we);
Llqr = (2.17)/(we);
Lmq = (42.46)/we;

% For array - Excel Result
k = 1;
```

```
for wr = 3000:10:3500
wr_rpm = wr;
wr = wr*2*pi / 60; % Convertion of omega to rad/sec

% Equation Solver
syms Iqss1 Iqss2 fqss1 fqss2 Iqrr1 Iqrr2 fqrr1 fqrr2...
 Idrr1 Idrr2 fdrr1 fdrr2

[Iqss1 Iqss2 fqss1 fqss2 Iqrr1 Iqrr2 fqrr1 fqrr2 Idrr1...
 Idrr2 fdrr1 fdrr2]...
= solve (...
Vqss1 - rqs*Iqss1 + we*fqss2 ==0,...
Vqss2 - rqs*Iqss2 - we*fqss1 ==0,...
-fdrr1*wr + rqr*Iqrr1 - we*fqrr2 == 0,...
-fdrr2*wr + rqr*Iqrr2 + we*fqrr1 == 0,...
fqrr1*wr + rqr*Idrr1 - we*fdrr2 == 0,...
fqrr2*wr + rqr*Idrr2 + we*fdrr1 ==0,...
fqss1 - Llqs*Iqss1 - Lmq*(Iqss1 + Iqrr1) == 0,...
fqss2 - Llqs*Iqss2 - Lmq*(Iqss2 + Iqrr2) == 0,...
fqrr1 - Llqr*Iqrr1 - Lmq*(Iqss1 + Iqrr1) == 0,...
fqrr2 - Llqr*Iqrr2 - Lmq*(Iqss2 + Iqrr2) == 0,...
fdrr1 - Llqr*Idrr1 - Lmq*(Idrr1) == 0,...
fdrr2 - Llqr*Idrr2 - Lmq*(Idrr2) == 0,...
Iqss1, Iqss2, fqss1, fqss2, Iqrr1, Iqrr2, fqrr1, fqrr2,...
 Idrr1, Idrr2, fdrr1, fdrr2);

% Accumulation of Real and Imaginery Results

fdrr1 = double (fdrr1);
fdrr2 = double (fdrr2);
fqss1 = double (fqss1);
fqss2 = double (fqss2);
fqrr1 = double (fqrr1);
fqrr2 = double (fqrr2);

Idrr1 = double (Idrr1);
```

```
Idrr2 = double (Idrr2);
Iqss1 = double (Iqss1);
Iqss2 = double (Iqss2);
Iqrr1 = double (Iqrr1);
Iqrr2 = double (Iqrr2);

fdrr = fdrr1 + 1i*fdrr2;
fqss = fqss1 + 1i*fqss2;
fqrr = fqrr1 + 1i*fqrr2;

Idrr = double(Idrr1) + 1i*double(Idrr2);
Iqss = double(Iqss1) + 1i*double(Iqss2);
Iqrr = double(Iqrr1) + 1i*double(Iqrr2);

Vqss = double(Vqss1) + 1i*double(Vqss2);

% Electrical Power
PVqss = abs(real((Vqss) .* conj(Iqss)))/2;
array_PVqss(k) =  PVqss;

% Mechanical power
Pdr = real((wr*fqrr) .* conj(Idrr))/2;
Pqr = real((wr*fdrr) .* conj(Iqrr))/2;
array_Pdr(k) =  Pdr;
array_Pqr(k) =  Pqr;

% losses
P_rdr = abs(Idrr)^2*rqr/2;
P_rqs = abs(Iqss)^2*rqs/2;
P_rqr = abs(Iqrr)^2*rqr/2;
array_Prdr(k) =  P_rdr;
array_Prqs(k) =  P_rqs;
array_Prqr(k) =  P_rqr;

% Power In
Pin = PVqss;
array_Pin(k) = Pin;
```

```
% Power out
Pout = - Pqr + Pdr;
array_Pout(k) = Pout;

% Total Losses
TLosses = P_rdr + P_rqs + P_rqr;
array_TLosses(k) = TLosses;

% NIL Check - Power Balance ?
Check = Pin - Pout - TLosses;
array_Check(k) = Check;

% Efficiency
Eff = Pout*100 / Pin;
array_Eff(k) = Eff;

%Torque
T = (2*(Pdr - Pqr))/wr;
array_Torque(k) = T;

% Accumulation of results into an array
% to write xls file
array_wr(k) = wr;
array_wrrpm(k) = wr_rpm;
array_Iqss(k) = (Iqss)/sqrt(2);
array_Iqrr(k) = (Iqrr)/sqrt(2);
array_Idrr(k) = (Idrr)/sqrt(2);
array_fqss(k) = (fqss)/sqrt(2);
array_fqrr(k) = (fqrr)/sqrt(2);
array_fdrr(k) = (fdrr)/sqrt(2);

array_magIqss(k) = abs(Iqss)/sqrt(2);
array_magIqrr(k) = abs(Iqrr)/sqrt(2);
array_magIdrr(k) = abs(Idrr)/sqrt(2);
array_magfqss(k) = abs(fqss)/sqrt(2);
array_magfqrr(k) = abs(fqrr)/sqrt(2);
```

```
array_magfdrr(k) = abs(fdrr)/sqrt(2);

k=k+1;
end

% Base Units
Pb = 248.6666667;
Vb = 162.6345597;
wb = 377;
Ib = 3.057980631/sqrt(2);
Zb = 53.18364611;
Teb = 1.319186561;
fb = 0.431391405;

xlswrite('SinglePhase.xlsx',[array_wrrpm; array_wr;...
array_magIqss/Ib; array_magIqrr/Ib;...
array_magIdrr/Ib;...
array_PVqss/Pb; array_Pdr/Pb; array_Pqr/Pb;...
array_Prdr/Pb;...
array_Prqs/Pb; array_Prqr/Pb; array_Pin/Pb;...
array_Pout/Pb; array_TLosses/Pb;...
array_Eff; array_Torque/Teb; array_Check]);
```

Appendix C EQUATION SOLVER CODE FOR TWO WINDING MACHINE

```
%%%%%%%%%%%%%%%%%%%%%%%%%%%%%%%%%%%%%%%%%%%%%%%%%%%%%%%%%%%%%%%%
% File Name: TwoPhaseOperation.m
%%%%%%%%%%%%%%%%%%%%%%%%%%%%%%%%%%%%%%%%%%%%%%%%%%%%%%%%%%%%%%%%
% This file constains the machine equations
% to solve for Two Winding Machine motoring
% operation after the machine's auxiliary
% winding has been disconnected
%%%%%%%%%%%%%%%%%%%%%%%%%%%%%%%%%%%%%%%%%%%%%%%%%%%%%%%%%%%%%%%%

clear all;
clc;

% Turns Ratio
Ndq = 1.18;
Nqd = 1/Ndq;

% Machine Voltage condition
Vqss1 = sqrt(2)*115;
Vqss2 = 0;

% Excitation Frequency
we = 377;

% Machine Resistances
rqs = 1.2;
rqr = 2.4;
rds = 7.5;
rdr = Ndq*Ndq*rqr;

% Machine Inductances
```

```
Llqs = (3.74)/(we);
Llqr = (2.17)/(we);
Lmq = (42.46)/we;
Llds = (7.9652)/(we);
Lldr = (3.0215)/we;
Lmd = (59.12)/we;

% For array - Excel Result
k = 1;

% Run Capacitor Value
Cx = 20e-6;

for wr = 3000:2.5:3550;
wr_rpm = wr;
wr = wr*2*pi/60; % Convertion of omega to rad/sec

% Equation Solver
syms Vdss1 Vdss2 Iqss1 Iqss2 fqss1 fqss2 Iqrr1...
Iqrr2 fqrr1 fqrr2 Idss1 Idss2 Idrr1 Idrr2 fdss1...
fdss2 fdrr1 fdrr2

[Vdss1 Vdss2 Iqss1 Iqss2 fqss1 fqss2 Iqrr1 Iqrr2 fqrr1...
fqrr2 Idss1 Idss2 Idrr1 Idrr2 fdss1 fdss2 fdrr1 fdrr2]...
= solve (...
Vqss1 - rqs*Iqss1 + we*fqss2 ==0, ...
Vqss2 - rqs*Iqss2 - we*fqss1 ==0, ...
Vdss1 - rds*Idss1 + we*fdss2 ==0, ...
Vdss2 - rds*Idss2 - we*fdss1 ==0, ...
-Nqd*fdrr1*wr + rqr*Iqrr1 - we*fqrr2 == 0, ...
-Nqd*fdrr2*wr + rqr*Iqrr2 + we*fqrr1 == 0, ...
Ndq*fqrr1*wr + rdr*Idrr1 - we*fdrr2 == 0, ...
Ndq*fqrr2*wr + rdr*Idrr2 + we*fdrr1 ==0, ...
fqss1 - Llqs*Iqss1 - Lmq*(Iqss1 + Iqrr1) == 0, ...
fqss2 - Llqs*Iqss2 - Lmq*(Iqss2 + Iqrr2) == 0, ...
fqrr1 - Llqr*Iqrr1 - Lmq*(Iqss1 + Iqrr1) == 0, ...
fqrr2 - Llqr*Iqrr2 - Lmq*(Iqss2 + Iqrr2) == 0, ...
```

```
fdss1 - Llds*Idss1 - Lmd*(Idss1 + Idrr1) == 0, ...
fdss2 - Llds*Idss2 - Lmd*(Idss2 + Idrr2) == 0, ...
fdrr1 - Lldr*Idrr1 - Lmd*(Idss1 + Idrr1) == 0, ...
fdrr2 - Lldr*Idrr2 - Lmd*(Idss2 + Idrr2) == 0, ...
Idss1 + we*Cx*Vqss2 - we*Cx*Vdss2 == 0, ...
Idss2 - we*Cx*Vqss1 + we*Cx*Vdss1 == 0, ...
Vdss1, Vdss2, Iqss1, Iqss2, fqss1, fqss2, Iqrr1,...
Iqrr2,fqrr1, fqrr2, Idss1, Idss2, Idrr1, Idrr2,...
fdss1, fdss2,fdrr1, fdrr2);

% Accumulation of Real and Imaginery Results
fdss1 = double (fdss1);
fdss2 = double (fdss2);
fdrr1 = double (fdrr1);
fdrr2 = double (fdrr2);
fqss1 = double (fqss1);
fqss2 = double (fqss2);
fqrr1 = double (fqrr1);
fqrr2 = double (fqrr2);

Idss1 = double (Idss1);
Idss2 = double (Idss2);
Idrr1 = double (Idrr1);
Idrr2 = double (Idrr2);
Iqss1 = double (Iqss1);
Iqss2 = double (Iqss2);
Iqrr1 = double (Iqrr1);
Iqrr2 = double (Iqrr2);

fdss = fdss1 + 1i*fdss2;
fdrr = fdrr1 + 1i*fdrr2;
fqss = fqss1 + 1i*fqss2;
fqrr = fqrr1 + 1i*fqrr2;

Idss = double(Idss1) + 1i*double(Idss2);
Idrr = double(Idrr1) + 1i*double(Idrr2);
Iqss = double(Iqss1) + 1i*double(Iqss2);
```

```
Iqrr = double(Iqrr1) + 1i*double(Iqrr2);

Vdss = double(Vdss1) + 1i*double(Vdss2);
Vqss = double(Vqss1) + 1i*double(Vqss2);
array_magVqss(k) = abs(Vqss)/sqrt(2);
array_magVdss(k) = abs(Vdss)/sqrt(2);

% Electrical Power
PVdss = abs(real((Vdss) .* conj(Idss)))/2;
PVqss = abs(real((Vqss) .* conj(Iqss)))/2;
array_PVqss(k) =  PVqss;
array_PVdss(k) =  PVdss;

% Mechanical power
Pdr = real((Ndq*wr*fqrr) .* conj(Idrr))/2;
Pqr = real((Nqd*wr*fdrr) .* conj(Iqrr))/2;
array_Pdr(k) =  Pdr;
array_Pqr(k) =  Pqr;

% losses
P_rds = abs(Idss)^2*rds/2;
P_rdr = abs(Idrr)^2*rdr/2;
P_rqs = abs(Iqss)^2*rqs/2;
P_rqr = abs(Iqrr)^2*rqr/2;
array_Prds(k) =  P_rds;
array_Prdr(k) =  P_rdr;
array_Prqs(k) =  P_rqs;
array_Prqr(k) =  P_rqr;

% Total Losses
TLosses = P_rds + P_rdr + P_rqs + P_rqr;
array_TLosses(k) = TLosses;

% Power In
Pin = PVqss + PVdss;
array_Pin(k) = Pin;
```

```
% Power out
Pout = - Pqr + Pdr;
array_Pout(k) = Pout;

% NIL Check - Power Balance ?
Check = Pin - Pout - TLosses;
array_Check(k) = Check;

% Efficiency
Eff = Pout*100 / Pin;
array_Eff(k) = Eff;

%Torque
T = (2*(Pdr - Pqr))/wr;
array_Torque(k) = T;

% Accumulation of results into an array
% to write xls file
array_wr(k)=wr;
array_wrrpm(k)=wr_rpm;

array_Iqss(k) = (Iqss)/sqrt(2);
array_Iqrr(k) = (Iqrr)/sqrt(2);
array_Idss(k) = (Idss)/sqrt(2);
array_Idrr(k) = (Idrr)/sqrt(2);
array_fqss(k) = (fqss)/sqrt(2);
array_fqrr(k) = (fqrr)/sqrt(2);
array_fdss(k) = (fdss)/sqrt(2);
array_fdrr(k) = (fdrr)/sqrt(2);

array_magIqss(k) = abs(Iqss)/sqrt(2);
array_magIqrr(k) = abs(Iqrr)/sqrt(2);
array_magIdss(k) = abs(Idss)/sqrt(2);
array_magIdrr(k) = abs(Idrr)/sqrt(2);
array_magfqss(k) = abs(fqss)/sqrt(2);
array_magfqrr(k) = abs(fqrr)/sqrt(2);
array_magfdss(k) = abs(fdss)/sqrt(2);
```

```
array_magfdrr(k) = abs(fdrr)/sqrt(2);

k=k+1;
end
% Base Units
Pb = 248.6666667;
Vb = 162.6345597;
wb = 377;

Ib = 3.057980631/sqrt(2);
Zb = 53.18364611;
Teb = 1.319186561;
fb = 0.431391405;

xlswrite('TwoPhase.xlsx',[array_wrrpm; array_wr;...
array_magIqss/Ib; array_magIqrr/Ib; ...
array_magIdss/Ib; array_magIdrr/Ib; ...
array_PVqss/Pb; array_Pdr/Pb; array_Pqr/Pb;...
array_Prds/Pb; array_Prdr/Pb;array_Prqs/Pb;...
array_Prqr/Pb; array_Pin/Pb; array_Pout/Pb;...
array_TLosses/Pb; ...
array_Eff; array_Torque/Teb; array_Check]);
```

Appendix D DYNAMIC SIMULATION FOR SINGLE AND TWO WINDING MACHINE

```
%%%%%%%%%%%%%%%%%%%%%%%%%%%%%%%%%%%%%%%%%%%%%%%%%%%%%%%%%%%%%%%%
% File Name: OneWindingFunction.m
%%%%%%%%%%%%%%%%%%%%%%%%%%%%%%%%%%%%%%%%%%%%%%%%%%%%%%%%%%%%%%%%
% This file calls the following functions
% LineStart_StartCap: Machine Equation Solver with
% only start capacitor
% LineStart_NoCap: Machine Equations Solver with
% only ine winding
%%%%%%%%%%%%%%%%%%%%%%%%%%%%%%%%%%%%%%%%%%%%%%%%%%%%%%%%%%%%%%%%

clc;
clear all;

% Excitation Frequency
we = 377;

% Turns Ratio
Ndq = 1.18;
Nqd = 1/Ndq;

% Machine Inductances
Llqs = (3.74)/(we);
Llqr = (2.17)/(we);
Lmq = (42.46)/we;
Llds = (7.9652)/(we);
Lldr = (3.0215)/we;
Lmd = (59.12)/we;
Lqs = Llqs + Lmq;
Lqr = Llqr + Lmq;
Lds = Llds + Lmd;
```

```
Ldr = Lldr + Lmd;

yi1 = [0 0 0 0 0 0];
[t1,y1] = ode45(@LineStart_StartCap,[0 0.2974],yi1);
yi2 = [y1(end,1) y1(end,2) y1(end,4) y1(end,5)];
[t2,y2] = ode45(@LineStart_NoCap,[0.2974 1],yi2);

Tem1 = 2*(y1(:,2).*((Lds*y1(:,4) -...
Lmd*y1(:,3))/(Lds*Ldr-Lmd^2)))-2.*y1(:,4)...
.*((Lqs*y1(:,2) - Lmq*y1(:,1))...
/(Lqs*Lqr - Lmq^2));
Tem2 = ((2)*(y2(:,2).*((y2(:,3))/(Llqr + Lmq)) -...
 y2(:,3).*(((Llqs + Lmq)*y2(:,2) - Lmq*y2(:,1))..
 /(Llqs*Llqr + Lmq*(Llqs + Llqr)))));

iqs1 = (Lmq*y1(:,2) - Lqr*y1(:,1))/(Lmq^2 - Lqs*Lqr);
iqs2 = ((Llqr + Lmq)*y2(:,1) - Lmq*y2(:,2))...
/(Llqs*Llqr + Lmq*(Llqs + Llqr));

ids1 = (Lmd*y1(:,4) - Ldr*y1(:,3))/(Lmd^2 - Lds*Ldr);
ids2 = 0*y2(:,4);

Pout1 = 0.5*Tem1.*y1(:,5);
Pout2 = 0.5*Tem2.*y2(:,4);

% Base Units
Pb = 248.6666667;
Vb = 115;
wb = 377;
Ib = Pb/Vb;
Zb = Vb/Ib;
Teb = (2*Pb)/wb;
fb = Vb/wb;

figure();

subplot(4,1,1)
```

```
plot(t1,y1(:,5));
hold on;
plot(t2,y2(:,4))
xlabel('Time');
title('Electrical Rotor Speed (SS RMS: 361.28 rad/sec)');

subplot(4,1,2)
plot(t1,iqs1/Ib);
hold on;
plot(t2,iqs2/Ib)
xlabel('Time');
title('Q Axis Stator Current (SS RMS: 2.44 p.u.)');

subplot(4,1,3)
plot(t1,ids1/Ib);
hold on;
plot(t2,ids2/Ib)
xlabel('Time');
title('D Axis Stator Current (SS RMS: 0 p.u.)');

subplot(4,1,4)
plot(t1,Tem1/Teb);
hold on;
plot(t2,Tem2/Teb)
xlabel('Time');
title('Torque (SS RMS: 1.04 p.u.)');

% Rotor Flux plot

figure();
plot(y1(:,2),y1(:,4));
hold on;
plot(y2(:,2),y2(:,3));
xlabel('Q Axis Rotor Flux');
ylabel('D Axis Rotor Flux');
title('Rotor flux plot (p.u.)');
limits = [-0.5 0.5 -0.5 0.5];
```

```
axis(limits);

%%%%%%%%%%%%%%%%%%%%%%%%%%%%%%%%%%%%%%%%%%%%%%%%%%%%%%%%%%%%
% File Name: LineStart_StartCap.m
%%%%%%%%%%%%%%%%%%%%%%%%%%%%%%%%%%%%%%%%%%%%%%%%%%%%%%%%%%%%
% Function file which is Machine Equation Solver
% with only start capacitor
%%%%%%%%%%%%%%%%%%%%%%%%%%%%%%%%%%%%%%%%%%%%%%%%%%%%%%%%%%%%

function dy = LineStart_StartCap(t,y)

% Excitation Frequency
we = 377;

% Turns Ratio
Ndq = 1.18;
Nqd = 1/Ndq;

% Input Voltage
vqs = 115*sqrt(2)*cos(we*t);

% Machine Resistances
rqs = 1.2;
rqr = 2.4;
rds = 7.5;
rdr = Ndq*Ndq*rqr;

% Inductances
Llqs = (3.74)/(we);
Llqr = (2.17)/(we);
Lmq = (42.46)/we;
Llds = (7.9652)/(we);
Lldr = (3.0215)/we;
Lmd = (59.12)/we;
Lqs = Llqs + Lmq;
Lqr = Llqr + Lmq;
Lds = Llds + Lmd;
```

```
Ldr = Lldr + Lmd;
% Only Start Capacitor
Cx = 180*1e-6;
% Start and Run Capacitor
% Cx = (180+20)*1e-6;
% Moment of Intertia
J = 0.01;

% Load Torque
wr_rated = 1725*(2*pi)*(1/60);
Pout = 247.2529;
% Pout = 252.7732;
T_rated = Pout/wr_rated;
Tload_k = T_rated/(wr_rated*wr_rated*2*2);

dy = zeros(6,1);
dy(1) = vqs - rqs*((Lmq*y(2) - Lqr*y(1))...
/(Lmq^2 - Lqs*Lqr));
dy(2) = Nqd*y(5)*y(4) - rqr*((Lqs*y(2) -...
 Lmq*y(1))/(Lqs*Lqr - Lmq^2));
dy(3) = y(6) - rds*((Lmd*y(4) - Ldr*y(3))...
/(Lmd^2 - Lds*Ldr));
dy(4) = - Ndq*y(5)*y(2) - rdr*((Lds*y(4)...
 - Lmd*y(3))/(Lds*Ldr - Lmd^2));
dy(5) = (2/J)*(2*Ndq*(y(2)*((Lds*y(4) - ...
Lmd*y(3))/(Lds*Ldr - Lmd^2)))-2*Nqd*y(4)*...
((Lqs*y(2) - Lmq*y(1))/(Lqs*Lqr - Lmq^2))...
 - 1*Tload_k*(y(5))^2);
dy(6) = - 115*sqrt(2)*we*sin(we*t) - (1/Cx)...
*((Lmd*y(4) - Ldr*y(3))/(Lmd^2 - Lds*Ldr));

% y(1) = fqs
% y(2) = fqr
% y(3) = fds
% y(4) = fdr
% y(5) = wr
% y(6) = vds
```

```
% iqs = (Lmq*y(2) - Lqr*y(1))/(Lmq^2 - Lqs*Lqr);
% iqr = (Lqs*y(2) - Lmq*y(1))/(Lqs*Lqr - Lmq^2);
% ids = (Lmd*y(4) - Ldr*y(3))/(Lmd^2 - Lds*Ldr);
% idr = (Lds*y(4) - Lmd*y(3))/(Lds*Ldr - Lmd^2);

end

%%%%%%%%%%%%%%%%%%%%%%%%%%%%%%%%%%%%%%%%%%%%%%%%%%%%%%%%%%%%
% File Name: LineStart_NoCap.m
%%%%%%%%%%%%%%%%%%%%%%%%%%%%%%%%%%%%%%%%%%%%%%%%%%%%%%%%%%%%
% Function file which is Machine Equation Solver
% with only one active winding
%%%%%%%%%%%%%%%%%%%%%%%%%%%%%%%%%%%%%%%%%%%%%%%%%%%%%%%%%%%%

function dy = LineStart_NoCap(t,y)

% Excitation Frequency
we = 377;

% Input Voltage
vqs = 115*sqrt(2)*cos(we*t);

% Machine Resistances
rqs = 1.2;
rqr = 2.4;

% Machine Inductances
Llqs = (3.74)/(we);
Llqr = (2.17)/(we);
Lmq = (42.46)/we;

% Moment of Intertia
J = 0.001;

% Load Torque
wr_rated = 3450*(2*pi)*(1/60);
```

```
Pout = 247.2529;
T_rated = Pout/wr_rated;
Tload_k = T_rated/(wr_rated^2);

dy = zeros(4,1);
dy(1) = vqs - rqs*(((Llqr + Lmq)*y(1) - ...
Lmq*y(2))/(Llqs*Llqr + Lmq*(Llqs + Llqr)));
dy(2) = y(3)*y(4) - rqr*(((Llqs + Lmq)*y(2) ...
- Lmq*y(1))/(Llqs*Llqr + Lmq*(Llqs + Llqr)));
dy(3) = - y(2)*y(4) - rqr*((y(3))/(Llqr + Lmq));
dy(4) = (2/J)*((2)*(y(2)*((y(3))/(Llqr + Lmq))...
 - y(3)*(((Llqs + Lmq)*y(2) - Lmq*y(1))...
 /(Llqs*Llqr + Lmq*(Llqs + Llqr)))) -...
  2*Tload_k*(y(4))^2);

% y(1) = fqs
% y(2) = fqr
% y(3) = fdr
% y(4) = wr

% idr = (y(3))/(Llqr + Lmq);
% iqs = ((Llqr + Lmq)*y(1) - Lmq*y(2))...
/(Llqs*Llqr + Lmq*(Llqs + Llqr));
% iqr = ((Llqs + Lmq)*y(2) - Lmq*y(1))...
/(Llqs*Llqr + Lmq*(Llqs + Llqr));

end

%%%%%%%%%%%%%%%%%%%%%%%%%%%%%%%%%%%%%%%%%%%%%%%%%%%%%%%%%%%%
% File Name: TwoWindingFunction.m
%%%%%%%%%%%%%%%%%%%%%%%%%%%%%%%%%%%%%%%%%%%%%%%%%%%%%%%%%%%%
% This file calls the following functions
% LineStart_StartCap: Machine Equation Solver with
% only start + run capacitor
% LineStart_RunCap: Machine Equations Solver with
% run capacitor only
%%%%%%%%%%%%%%%%%%%%%%%%%%%%%%%%%%%%%%%%%%%%%%%%%%%%%%%%%%%%
```

```
clc;
clear all;

% Excitation Frequency
we = 377;

% Turns Ratio
Ndq = 1.18;
Nqd = 1/Ndq;

% Machine Inductances
Llqs = (3.74)/(we);
Llqr = (2.17)/(we);
Lmq = (42.46)/we;
Llds = (7.9652)/(we);
Lldr = (3.0215)/we;
Lmd = (59.12)/we;
Lqs = Llqs + Lmq;
Lqr = Llqr + Lmq;
Lds = Llds + Lmd;
Ldr = Lldr + Lmd;

yi1 = [0 0 0 0 0 0];
[t1,y1] = ode45(@LineStart_StartCap,[0 0.2974],yi1);
yi2 = [y1(end,1) y1(end,2) y1(end,3) y1(end,4) ...
y1(end,5) y1(end,6)];
[t2,y2] = ode45(@LineStart_RunCap,[0.2974 1],yi2);

Tem1 = 2*y1(:,2).*((Lds*y1(:,4) - Lmd*y1(:,3))...
/(Lds*Ldr-Lmd^2))-2...
.*y1(:,4).*((Lqs*y1(:,2) - Lmq*y1(:,1))/...
(Lqs*Lqr - Lmq^2));
Tem2 = 2*y2(:,2).*((Lds*y2(:,4) - Lmd*y2(:,3))/(Lds*Ldr-...
Lmd^2))-2.*y2(:,4).*((Lqs*y2(:,2) - Lmq*y2(:,1))/...
(Lqs*Lqr - Lmq^2));
```

```
iqs1 = (Lmq*y1(:,2) - Lqr*y1(:,1))/(Lmq^2 - Lqs*Lqr);
iqs2 = (Lmq*y2(:,2) - Lqr*y2(:,1))/(Lmq^2 - Lqs*Lqr);

ids1 = (Lmd*y1(:,4) - Ldr*y1(:,3))/(Lmd^2 - Lds*Ldr);
ids2 = (Lmd*y2(:,4) - Ldr*y2(:,3))/(Lmd^2 - Lds*Ldr);

% Base Units
Pb = 248.6666667;
Vb = 115;
wb = 377;
Ib = Pb/Vb;
Zb = Vb/Ib;
Teb = (2*Pb)/wb;
fb = Vb/wb;

figure();

subplot(4,1,1)
plot(t1,y1(:,5));
hold on;
plot(t2,y2(:,5))
xlabel('Time');
title('Electrical Rotor Speed (SS RMS: 364.16 rad/sec)');

subplot(4,1,2)
plot(t1,iqs1/Ib);
hold on;
plot(t2,iqs2/Ib)
xlabel('Time');
title('Q Axis Stator Current (SS RMS: 1.82 p.u.)');

subplot(4,1,3)
plot(t1,ids1/Ib);
hold on;
plot(t2,ids2/Ib)
xlabel('Time');
title('D Axis Stator Current (SS RMS: 0.59 p.u.)');
```

```
subplot(4,1,4)
plot(t1,Tem1/Teb);
hold on;
plot(t2,Tem2/Teb)
xlabel('Time');
title('Torque (SS RMS: 1.04 p.u.)');

% Rotor Flux plot

figure();
plot(y1(:,2),y1(:,4));
hold on;
plot(y2(:,2),y2(:,4));
xlabel('Q Axis Rotor Flux');
ylabel('D Axis Rotor Flux');
title('Rotor flux plot (p.u.)');

limits = [-0.5 0.5 -0.5 0.5];
axis(limits);

%%%%%%%%%%%%%%%%%%%%%%%%%%%%%%%%%%%%%%%%%%%%%%%%%%%
% File Name: LineStart_RunCap.m
%%%%%%%%%%%%%%%%%%%%%%%%%%%%%%%%%%%%%%%%%%%%%%%%%%%
% Function file which is Machine Equation Solver
% with only run capacitor
%%%%%%%%%%%%%%%%%%%%%%%%%%%%%%%%%%%%%%%%%%%%%%%%%%%

function dy = LineStart_RunCap(t,y)

% Excitation Frequency
we = 377;

% Turns Ratio
Ndq = 1.18;
Nqd = 1/Ndq;
```

```
% Input Voltage
vqs = 115*sqrt(2)*cos(we*t);

% Machine Resistances
rqs = 1.2;
rqr = 2.4;
rds = 7.5;
rdr = Ndq*Ndq*rqr;

% Inductances
Llqs = (3.74)/(we);
Llqr = (2.17)/(we);
Lmq = (42.46)/we;
Llds = (7.9652)/(we);
Lldr = (3.0215)/we;
Lmd = (59.12)/we;
Lqs = Llqs + Lmq;
Lqr = Llqr + Lmq;
Lds = Llds + Lmd;
Ldr = Lldr + Lmd;
Cx = 20*1e-6;
% Moment of Intertia
J = 0.01;

% Load Torque
wr_rated = 1725*(2*pi)*(1/60);
Pout = 252.7732;
T_rated = Pout/wr_rated;
Tload_k = T_rated/(wr_rated*wr_rated*2*2);

dy = zeros(6,1);
dy(1) = vqs - rqs*((Lmq*y(2) - Lqr*y(1))/...
(Lmq^2 - Lqs*Lqr));
dy(2) = Nqd*y(5)*y(4) - rqr*((Lqs*y(2) - ...
Lmq*y(1))/(Lqs*Lqr - Lmq^2));
dy(3) = y(6) - rds*((Lmd*y(4) - Ldr*y(3))...
/(Lmd^2 - Lds*Ldr));
```

```
dy(4) = - Ndq*y(5)*y(2) - rdr*((Lds*y(4) -...
 Lmd*y(3))/(Lds*Ldr - Lmd^2));
dy(5) = (2/J)*(2*Ndq*(y(2)*((Lds*y(4) -...
 Lmd*y(3))/(Lds*Ldr - Lmd^2)))-2*Nqd*y(4)...
 *((Lqs*y(2) - Lmq*y(1))/(Lqs*Lqr - Lmq^2))...
  - 1*Tload_k*(y(5))^2);
dy(6) = - 115*sqrt(2)*we*sin(we*t) - (1/Cx)...
*((Lmd*y(4) - Ldr*y(3))/(Lmd^2 - Lds*Ldr));

% y(1) = fqs
% y(2) = fqr
% y(3) = fds
% y(4) = fdr
% y(5) = wr
% y(6) = vds

% iqs = (Lmq*y(2) - Lqr*y(1))/(Lmq^2 - Lqs*Lqr);
% iqr = (Lqs*y(2) - Lmq*y(1))/(Lqs*Lqr - Lmq^2);
% ids = (Lmd*y(4) - Ldr*y(3))/(Lmd^2 - Lds*Ldr);
% idr = (Lds*y(4) - Lmd*y(3))/(Lds*Ldr - Lmd^2);

end
```

Appendix E OPTIMIZATION CODE FOR FIXED FREQUENCY OPERATION

```
%%%%%%%%%%%%%%%%%%%%%%%%%%%%%%%%%%%%%%%%%%%%%%%%%%%%%%%%%%%%%%%%%%%%%%%%
% File Name: MachineParameters.m
%%%%%%%%%%%%%%%%%%%%%%%%%%%%%%%%%%%%%%%%%%%%%%%%%%%%%%%%%%%%%%%%%%%%%%%%
% This file contains the parameters of the machine
% under test
%%%%%%%%%%%%%%%%%%%%%%%%%%%%%%%%%%%%%%%%%%%%%%%%%%%%%%%%%%%%%%%%%%%%%%%%

% Machine's parameters
fe = 60;          % Excitation Frequency Hz
we = 2*pi*fe;     % Excitation Frequency rad/sec
% Turns Ratio
Ndq = 1.18;
Nqd = 1/ Ndq;
% D: Auxiliary Winding
% Q: Main Winding
% Machine Resistances ohms
rqs = 1.2;
rqr = 2.4;
rds = 7.5;
rdr = Ndq*Ndq*rqr;
% Machine Inductances Henries
Llqs = (3.74)/we;
Llqr = (2.17)/we;
Lmq = (42.46)/we;
Llds = (7.9652)/we;
Lldr = (3.0215)/we;
Lmd = (59.12)/we;
Lds = Llds + Lmd;
Ldr = Lldr + Lmd;
Lqs = Llqs + Lmq;
```

```
Lqr = Llqr + Lmq;
% Variable Assignment
% Q Winding Voltages
% x(1) Vqss1
% x(2) Vqss2
% D Winding Voltages
% x(3) Vdss1
% x(4) Vdss2
% Q Winding Stator Currents
% x(5) Iqss1
% x(6) Iqss2
% D Winding Stator Currents
% x(7) Idss1
% x(8) Idss2
% Q Winding Rotor Currents
% x(9) Iqrr1
% x(10) Iqrr2
% D Winding Rotor Currents
% x(11) Idrr1
% x(12) Idrr2
% Q Winding Stator Flux
% x(13) fqss1
% x(14) fqss2
% D Winding Stator Flux
% x(15) fdss1
% x(16) fdss2
% Q Winding Rotor Flux
% x(17) fqrr1
% x(18) fqrr2
% D Winding Rotor Flux
% x(19) fdrr1
% x(20) fdrr2
% Machine Equations
% Vqss1 - rqs*Iqss1 + we*fqss2 ==0, ...
% Vqss2 - rqs*Iqss2 - we*fqss1 ==0, ...
% Vdss1 - rds*Idss1 + we*fdss2 ==0, ...
% Vdss2 - rds*Idss2 - we*fdss1 ==0, ...
```

```
% -Nqd*fdrr1*wr + rqr*Iqrr1 - we*fqrr2 == 0, ...
% -Nqd*fdrr2*wr + rqr*Iqrr2 + we*fqrr1 == 0, ...
% Ndq*fqrr1*wr + rdr*Idrr1 - we*fdrr2 == 0, ...
% Ndq*fqrr2*wr + rdr*Idrr2 + we*fdrr1 ==0, ...
% fqss1 - Llqs*Iqss1 - Lmq*(Iqss1 + Iqrr1) == 0, ...
% fqss2 - Llqs*Iqss2 - Lmq*(Iqss2 + Iqrr2) == 0, ...
% fqrr1 - Llqr*Iqrr1 - Lmq*(Iqss1 + Iqrr1) == 0, ...
% fqrr2 - Llqr*Iqrr2 - Lmq*(Iqss2 + Iqrr2) == 0, ...
% fdss1 - Llds*Idss1 - Lmd*(Idss1 + Idrr1) == 0, ...
% fdss2 - Llds*Idss2 - Lmd*(Idss2 + Idrr2) == 0, ...
% fdrr1 - Lldr*Idrr1 - Lmd*(Idss1 + Idrr1) == 0, ...
% fdrr2 - Lldr*Idrr2 - Lmd*(Idss2 + Idrr2) == 0, ...

%%%%%%%%%%%%%%%%%%%%%%%%%%%%%%%%%%%%%%%%%%%%%%%%%%%%%%%%
% File Name: MaximizedEquation.m
%%%%%%%%%%%%%%%%%%%%%%%%%%%%%%%%%%%%%%%%%%%%%%%%%%%%%%%%
% This file contains the power output equation
% which has to be maximized
%%%%%%%%%%%%%%%%%%%%%%%%%%%%%%%%%%%%%%%%%%%%%%%%%%%%%%%%

function f = MaximizedEquation(x)
% Pe_op = Pdss + Pqss
f = (x(3)*x(7) + x(4)*x(8) + x(1)*x(5) + x(2)*x(6));
end

%%%%%%%%%%%%%%%%%%%%%%%%%%%%%%%%%%%%%%%%%%%%%%%%%%%%%%%%
% File Name: NonLinearConstraints.m
%%%%%%%%%%%%%%%%%%%%%%%%%%%%%%%%%%%%%%%%%%%%%%%%%%%%%%%%
% This file contains the non linear constraint
% equations
%%%%%%%%%%%%%%%%%%%%%%%%%%%%%%%%%%%%%%%%%%%%%%%%%%%%%%%%

function[c,ceq] = NonLinearConstraints(x)
MachineParameters;
c(1) = rqr*(x(9)^2) + rqr*(x(10)^2) + rdr*(x(11)^2)...
+ rdr*(x(12)^2) - 2*41.75;      % Rotor Losses
c(2) = x(3)^2 + x(4)^2 - 2*(115^2);% Vdss Voltage Limit
```

```
c(3) = x(1)^2 + x(2)^2 - 2*(115^2);% Vqss Voltage Limit
c(4) = rds*(x(7)^2) + rds*(x(8)^2) + rqs*(x(5)^2)...
+ rqs*(x(6)^2)- 2*33.56;        % D-Q Stator Winding Losses
ceq = [];
end

%%%%%%%%%%%%%%%%%%%%%%%%%%%%%%%%%%%%%%%%%%%%%%%%%%%%%%%%
% File Name: RunCode.m
%%%%%%%%%%%%%%%%%%%%%%%%%%%%%%%%%%%%%%%%%%%%%%%%%%%%%%%%
% This file contains the main code which calls
% the other files MaximizedEquation.m and
% NonLinearConstraints.m
%%%%%%%%%%%%%%%%%%%%%%%%%%%%%%%%%%%%%%%%%%%%%%%%%%%%%%%%

clear all;
clc;
options = optimset('Display','iter','TolFun',1e-18,...
'TolCon',1e-18);
MachineParameters;

Pb = 248.6666667;
Vb = 115;
wb = 377;

Ib = Pb/Vb;
Zb = Vb/Ib;
Teb = 2*Pb/wb;
fb = Vb/wb;

k = 1;                          % Array Count
for wr = 380:2:420              % Range of Rotor Speed

A1 = [];
b1 = [];
lb = -Inf;
ub = Inf;
A = [...% Linear Equality Machine Equations
```

```
1 0 0 0 -rqs 0 0 0 0 0 0 0 0 we 0 0 0 0 0 0;...
0 1 0 0 0 -rqs 0 0 0 0 0 0 0 -we 0 0 0 0 0 0 0;...
0 0 1 0 0 0 -rds 0 0 0 0 0 0 0 0 we 0 0 0 0;...
0 0 0 1 0 0 0 -rds 0 0 0 0 0 0 0 -we 0 0 0 0 0;...
0 0 0 0 0 0 0 0 rqr 0 0 0 0 0 0 0 0 -we -Nqd*wr 0;...
0 0 0 0 0 0 0 0 0 rqr 0 0 0 0 0 0 we 0 0 -Nqd*wr;...
0 0 0 0 0 0 0 0 0 0 rdr 0 0 0 0 0 Ndq*wr 0 0 -we;...
0 0 0 0 0 0 0 0 0 0 0 rdr 0 0 0 0 0 Ndq*wr we 0;...
0 0 0 0 -Llqs-Lmq 0 0 0 -Lmq 0 0 0 1 0 0 0 0 0 0 0;...
0 0 0 0 0 -Llqs-Lmq 0 0 0 -Lmq 0 0 0 1 0 0 0 0 0 0;...
0 0 0 0 -Lmq 0 0 0 -Llqr-Lmq 0 0 0 0 0 0 0 1 0 0 0;...
0 0 0 0 0 -Lmq 0 0 0 -Llqr-Lmq 0 0 0 0 0 0 0 1 0 0;...
0 0 0 0 0 0 -Llds-Lmd 0 0 0 -Lmd 0 0 0 1 0 0 0 0 0;...
0 0 0 0 0 0 0 -Llds-Lmd 0 0 0 -Lmd 0 0 0 1 0 0 0 0;...
0 0 0 0 0 0 -Lmd 0 0 0 -Lldr-Lmd 0 0 0 0 0 0 0 1 0;...
0 0 0 0 0 0 0 -Lmd 0 0 0 -Lldr-Lmd 0 0 0 0 0 0 0 1;...
0 1 0 0 0 0 0 0 0 0 0 0 0 0 0 0 0 0 0 0 0;...
];
B = [0; 0; 0; 0; 0; 0; 0; 0; 0; 0; 0; 0; 0; 0; 0; 0; 0];
x0 = [sqrt(2)*115;0;0;sqrt(2)*115;2;2;2;2;2;2;2;2;.1;.1;...
.1;.1;.1;.1;.1;.1];
x = fmincon(@MaximizedEquation,x0,A1,b1,A,B,lb,ub,...
@NonLinearConstraints,options);

% Variable assignment back to appropriate variables

Vqss = (x(1) + 1i*x(2))/sqrt(2);
Vdss = (x(3) + 1i*x(4))/sqrt(2);

Iqss = (x(5) + 1i*x(6))/ sqrt(2);
Idss = (x(7) + 1i*x(8))/ sqrt(2);
Iqrr = (x(9) + 1i*x(10))/ sqrt(2);
Idrr = (x(11) + 1i*x(12))/ sqrt(2);

Vdss_mag = sqrt(x(3)^2 + x(4)^2)/sqrt(2);
Vqss_mag = sqrt(x(1)^2 + x(2)^2)/sqrt(2);
Idss_mag = abs(Idss);
```

```
Iqss_mag = abs(Iqss);

% Loss Calculation
Ploss_rds = (rds*abs(Idss)^2);% Loss in D Stator R
Ploss_rqs = (rqs*abs(Iqss)^2);% Loss in Q Stator R
Ploss_rotor = (rdr*abs(Idrr)^2) + ...
(rqr*abs(Iqrr)^2);% Rotor Loss

PVdss = real((Vdss) .* conj(Idss));% D Winding Inverter P
PVqss = real((Vqss) .* conj(Iqss));% Q Winding Inverter P
Pdr = real((Ndq*wr*(x(17) + 1i*x(18))).*conj(-Idrr))/sqrt(2);
Pqr = real((Nqd*wr*(x(19) + 1i*x(20))).*conj(Iqrr))/sqrt(2);
Pinput = (Pqr + Pdr);% Mechanical Input Power
Poutput = (- PVdss - PVqss);% Electrical Output P
Efficiency = (Poutput)/(Pinput)*100;% Machine Efficiency
Check = Pqr + Pdr + PVdss + PVqss - Ploss_rds...
 - Ploss_rqs - Ploss_rotor;

% Save variables into arrays for record

array_check(k) = Check;
array_input(k) = Pinput;
array_output(k) = Poutput;
array_efficiency(k) = Efficiency;
array_losses(k) = Ploss_rds + Ploss_rqs + Ploss_rotor;
array_Vdssmag(k) = Vdss_mag;
array_Vqssmag(k) = Vqss_mag;
array_slip(k) = (2*pi*60 - wr) / (2*pi*60);
array_inverter1(k) = - PVqss;
array_inverter2(k) = - PVdss;
array_rds(k) = Ploss_rds;
array_rqs(k) = Ploss_rqs;
array_stator(k) = Ploss_rds+Ploss_rqs;
array_rotor(k) = Ploss_rotor;
array_Idssmag(k) = Idss_mag;
array_Iqssmag(k) = Iqss_mag;
angleVqs(k) = (angle(Vqss));
```

```
angleVds(k) = (angle(Vdss));
angleIqs(k) = (angle(Iqss));
angleIds(k) = (angle(Idss));
ValueVqs(k) = Vqss/Vb;
ValueVds(k) = Vdss/Vb;
ValueIqs(k) = Iqss/Ib;
ValueIds(k) = Idss/Ib;
k = k + 1;
end

% Write the data into Excel File
xlswrite('Data.xlsx',[array_slip;array_input;...
array_output;...
array_Vdssmag;array_Idssmag;angleVds;angleIds;...
array_Vqssmag;array_Iqssmag;angleVqs;angleIqs;...
array_inverter1;array_inverter2;array_efficiency;...
array_check]);
% Plot the Polar Plot of excitation conditions
plot1 = polar(angleVqs, array_Vqssmag/115,'*b');
hold on;
plot2 = polar(angleVds, array_Vdssmag/115,'*r');
hold on;
plot3 = polar(angleIds, array_Idssmag/5.2,'-r');
hold on;
plot4 = polar(angleIqs, array_Iqssmag/5.2,'-b');
set(plot3,'linewidth',2);
set(plot4,'linewidth',2);
```

Appendix F OPTIMIZATION CODE FOR VARIABLE FREQUENCY OPERATION

```
%%%%%%%%%%%%%%%%%%%%%%%%%%%%%%%%%%%%%%%%%%%%%%%%%%%%%%%%%%%%%%%%%%%%%%%%
% File Name: MachineParameters.m
%%%%%%%%%%%%%%%%%%%%%%%%%%%%%%%%%%%%%%%%%%%%%%%%%%%%%%%%%%%%%%%%%%%%%%%%
% This file contains the parameters of the machine
% under test
%%%%%%%%%%%%%%%%%%%%%%%%%%%%%%%%%%%%%%%%%%%%%%%%%%%%%%%%%%%%%%%%%%%%%%%%

% Machine's parameters
fe = 60;          % Excitation Frequency Hz
we = 2*pi*fe;     % Excitation Frequency rad/sec
% Turns Ratio
Ndq = 1.18;
Nqd = 1/ Ndq;
% D: Auxiliary Winding
% Q: Main Winding
% Machine Resistances ohms
rqs = 1.2;
rqr = 2.4;
rds = 7.5;
rdr = Ndq*Ndq*rqr;
% Machine Inductances Henries
Llqs = (3.74)/we;
Llqr = (2.17)/we;
Lmq = (42.46)/we;
Llds = (7.9652)/we;
Lldr = (3.0215)/we;
Lmd = (59.12)/we;
Lds = Llds + Lmd;
Ldr = Lldr + Lmd;
Lqs = Llqs + Lmq;
```

```
Lqr = Llqr + Lmq;
% Variable Assignment
% Q Winding Voltages
% x(1) Vqss1
% x(2) Vqss2
% D Winding Voltages
% x(3) Vdss1
% x(4) Vdss2
% Q Winding Stator Currents
% x(5) Iqss1
% x(6) Iqss2
% D Winding Stator Currents
% x(7) Idss1
% x(8) Idss2
% Q Winding Rotor Currents
% x(9) Iqrr1
% x(10) Iqrr2
% D Winding Rotor Currents
% x(11) Idrr1
% x(12) Idrr2
% Q Winding Stator Flux
% x(13) fqss1
% x(14) fqss2
% D Winding Stator Flux
% x(15) fdss1
% x(16) fdss2
% Q Winding Rotor Flux
% x(17) fqrr1
% x(18) fqrr2
% D Winding Rotor Flux
% x(19) fdrr1
% x(20) fdrr2
% Excitation Frwquency in rad/sec
% x(21)
% Machine Equations
% Vqss1 - rqs*Iqss1 + we*fqss2 ==0, ...
% Vqss2 - rqs*Iqss2 - we*fqss1 ==0, ...
```

```
% Vdss1 - rds*Idss1 + we*fdss2 ==0, ...
% Vdss2 - rds*Idss2 - we*fdss1 ==0, ...
% -Nqd*fdrr1*wr + rqr*Iqrr1 - we*fqrr2 == 0, ...
% -Nqd*fdrr2*wr + rqr*Iqrr2 + we*fqrr1 == 0, ...
% Ndq*fqrr1*wr + rdr*Idrr1 - we*fdrr2 == 0, ...
% Ndq*fqrr2*wr + rdr*Idrr2 + we*fdrr1 ==0, ...
% fqss1 - Llqs*Iqss1 - Lmq*(Iqss1 + Iqrr1) == 0, ...
% fqss2 - Llqs*Iqss2 - Lmq*(Iqss2 + Iqrr2) == 0, ...
% fqrr1 - Llqr*Iqrr1 - Lmq*(Iqss1 + Iqrr1) == 0, ...
% fqrr2 - Llqr*Iqrr2 - Lmq*(Iqss2 + Iqrr2) == 0, ...
% fdss1 - Llds*Idss1 - Lmd*(Idss1 + Idrr1) == 0, ...
% fdss2 - Llds*Idss2 - Lmd*(Idss2 + Idrr2) == 0, ...
% fdrr1 - Lldr*Idrr1 - Lmd*(Idss1 + Idrr1) == 0, ...
% fdrr2 - Lldr*Idrr2 - Lmd*(Idss2 + Idrr2) == 0, ...

%%%%%%%%%%%%%%%%%%%%%%%%%%%%%%%%%%%%%%%%%%%%%%%%%%%%%%%%%%%%
% File Name: MaximizedEquation.m
%%%%%%%%%%%%%%%%%%%%%%%%%%%%%%%%%%%%%%%%%%%%%%%%%%%%%%%%%%%%
% This file contains the power output equation
% which has to be maximized
%%%%%%%%%%%%%%%%%%%%%%%%%%%%%%%%%%%%%%%%%%%%%%%%%%%%%%%%%%%%

function f = MaximizedEquation(x)
% Pe_op = Pdss + Pqss
f = (x(3)*x(7) + x(4)*x(8) + x(1)*x(5) + x(2)*x(6));
end

%%%%%%%%%%%%%%%%%%%%%%%%%%%%%%%%%%%%%%%%%%%%%%%%%%%%%%%%%%%%
% File Name: NonLinearConstraints.m
%%%%%%%%%%%%%%%%%%%%%%%%%%%%%%%%%%%%%%%%%%%%%%%%%%%%%%%%%%%%
% This file contains the non linear constraint
% equations
%%%%%%%%%%%%%%%%%%%%%%%%%%%%%%%%%%%%%%%%%%%%%%%%%%%%%%%%%%%%

function[c,ceq] = NonLinearConstraints(x)

MachineParameters;
```

```
c(1) = rqr*(x(9)^2) + rqr*(x(10)^2) + rdr*(x(11)^2)...
+ rdr*(x(12)^2) - 2*41.75;% Rotor Losses within limits
c(2) = rds*(x(7)^2) + rds*(x(8)^2) + rqs*(x(5)^2)...
+ rqs*(x(6)^2) - 2*33.56;% Stator Losses within limits
c(3) = - x(21) + 0;% Positive Excitation frequency
c(4) = x(21) - x(22);% Stator Speed more than rotor speed
c(5) = (x(3)*x(7) + x(4)*x(8) + x(1)*x(5)...
+ x(2)*x(6));% Power Output less than zero
ceq(1) = x(1) - rqs*x(5) + x(21)*x(14);
ceq(2) = x(2) - rqs*x(6) - x(21)*x(13);
ceq(3) = x(3) - rds*x(7) + x(21)*x(16);
ceq(4) = x(4) - rds*x(8) - x(21)*x(15);
ceq(5) = -Nqd*x(19)*x(22) + rqr*x(9) - x(21)*x(18);
ceq(6) = -Nqd*x(20)*x(22) + rqr*x(10) + x(21)*x(17);
ceq(7) = Ndq*x(17)*x(22) + rdr*x(11) - x(21)*x(20);
ceq(8) = Ndq*x(18)*x(22) + rdr*x(12) + x(21)*x(19);
end

%%%%%%%%%%%%%%%%%%%%%%%%%%%%%%%%%%%%%%%%%%%%%%%%%%%%%%%%
% File Name: RunCode.m
%%%%%%%%%%%%%%%%%%%%%%%%%%%%%%%%%%%%%%%%%%%%%%%%%%%%%%%%
% This file contains the main code which calls
% the other files MaximizedEquation.m and
% NonLinearConstraints.m
%%%%%%%%%%%%%%%%%%%%%%%%%%%%%%%%%%%%%%%%%%%%%%%%%%%%%%%%

clear all;
clc;
options = optimset('Display','iter','TolFun',1e-18...
,'TolCon',1e-18);
MachineParameters;

k = 1;                          % Array Count
for wr = 100:10:400             % Range of Rotor Speed
A1 = [];
b1 = [];
```

```
lb = -Inf;
ub = Inf;
A = [...% Linear Equality Equations (Flux Equations)
0 0 0 0 -Llqs-Lmq 0 0 0 -Lmq 0 0 0 1 0 0 0 0 0 0 0 0 0;...
0 0 0 0 0 -Llqs-Lmq 0 0 0 -Lmq 0 0 0 1 0 0 0 0 0 0 0 0;...
0 0 0 0 -Lmq 0 0 0 -Llqr-Lmq 0 0 0 0 0 0 0 1 0 0 0 0 0;...
0 0 0 0 0 -Lmq 0 0 0 -Llqr-Lmq 0 0 0 0 0 0 0 1 0 0 0 0;...
0 0 0 0 0 0 -Llds-Lmd 0 0 0 -Lmd 0 0 0 1 0 0 0 0 0 0 0;...
0 0 0 0 0 0 0 -Llds-Lmd 0 0 0 -Lmd 0 0 0 1 0 0 0 0 0 0;...
0 0 0 0 0 0 -Lmd 0 0 0 -Lldr-Lmd 0 0 0 0 0 0 0 1 0 0 0;...
0 0 0 0 0 0 0 -Lmd 0 0 0 -Lldr-Lmd 0 0 0 0 0 0 0 1 0 0;...
0 0 0 0 0 0 0 0 0 0 0 0 0 0 0 0 0 0 0 0 0 0 1;...
0 1 0 0 0 0 0 0 0 0 0 0 0 0 0 0 0 0 0 0 0 0 0;...
];
B = [0; 0; 0; 0; 0; 0; 0; 0; wr; 0];
x0 = [sqrt(2)*115;0;0;sqrt(2)*115;2;2;2;2;2;2;2;.1;.1...
;.1;.1;.1;.1;.1;.1;wr;wr];
x = fmincon(@MaximizedEquation,x0,A1,b1,A,B,lb,ub,...
@NonLinearConstraints,options);

% Variable assignment back to appropriate variables

excitation_frequency = x(21);

Vqss = (x(1) + 1i*x(2))/sqrt(2);
Vdss = (x(3) + 1i*x(4))/sqrt(2);

Iqss = (x(5) + 1i*x(6))/ sqrt(2);
Idss = (x(7) + 1i*x(8))/ sqrt(2);
Iqrr = (x(9) + 1i*x(10))/ sqrt(2);
Idrr = (x(11) + 1i*x(12))/ sqrt(2);

fqss = abs((x(13) + 1i*x(14))/ sqrt(2));
fdss = abs((x(15) + 1i*x(16))/ sqrt(2));
fqrr = abs((x(17) + 1i*x(18))/ sqrt(2));
fdrr = abs((x(19) + 1i*x(20))/ sqrt(2));
```

```
Vdss_mag = sqrt(x(3)^2 + x(4)^2)/sqrt(2);
Vqss_mag = sqrt(x(1)^2 + x(2)^2)/sqrt(2);
Idss_mag = abs(Idss);
Iqss_mag = abs(Iqss);

% Loss Calculation
Ploss_rds = (rds*abs(Idss)^2);% Loss in D Stator R
Ploss_rqs = (rqs*abs(Iqss)^2);% Loss in Q Stator R
Ploss_rotor = (rdr*abs(Idrr)^2)+(rqr*abs(Iqrr)^2);% Rotor Loss

PVdss = real((Vdss) .* conj(Idss));% D Winding Inverter P
PVqss = real((Vqss) .* conj(Iqss));% Q Winding Inverter P
Pdr = real((Ndq*wr*(x(17) + 1i*x(18))).*conj(-Idrr))/sqrt(2);
Pqr = real((Nqd*wr*(x(19) + 1i*x(20))).*conj(Iqrr))/sqrt(2);
Pinput = (Pqr + Pdr);% Mechanical Input Power
Poutput = (- PVdss - PVqss);% Electrical Output Power
Efficiency = (Poutput)/(Pinput)*100;% Machine Efficiency
Check = Pqr + Pdr + PVdss + PVqss - Ploss_rds...
 - Ploss_rqs - Ploss_rotor;

S_ds = Vdss_mag*Idss_mag;% D Winding VA
S_qs = Vqss_mag*Iqss_mag;% Q Winding VA
Q_ds = sqrt(S_ds^2 - PVdss^2);% D Winding VAr
Q_qs = sqrt(S_qs^2 - PVqss^2);% Q Winding VAr

% Save variables into arrays for record

array_S_ds(k) = S_ds;
array_S_qs(k) = S_qs;
array_Q_ds(k) = Q_ds;
array_Q_Qs(k) = Q_qs;
array_fqss(k) = fqss;
array_fdss(k) = fdss;
array_fqrr(k) = fqrr;
array_fdrr(k) = fdrr;
array_check(k) = Check;
array_input(k) = Pinput;
```

```
array_output(k) = Poutput;
array_efficiency(k) = Efficiency;
array_losses(k) = Ploss_rds + Ploss_rqs + Ploss_rotor;
array_slip(k) = (2*pi*60 - wr) / (2*pi*60);
array_inverter1(k) = - PVqss;
array_inverter2(k) = - PVdss;
array_rds(k) = Ploss_rds;
array_rqs(k) = Ploss_rqs;
array_stator(k) = Ploss_rds+Ploss_rqs;
array_Vdssmag(k) = Vdss_mag;
array_Vqssmag(k) = Vqss_mag;
array_rotor(k) = Ploss_rotor;
array_Idssmag(k) = Idss_mag;
array_Iqssmag(k) = Iqss_mag;
angleVqs(k) = (angle(Vqss));
angleVds(k) = (angle(Vdss));
angleIqs(k) = (angle(Iqss));
angleIds(k) = (angle(Idss));
ValueVqs(k) = Vqss;
ValueVds(k) = Vdss;
ValueIqs(k) = Iqss;
ValueIds(k) = Idss;
array_excitation_frequency(k) = excitation_frequency;
array_rotor_speed(k) = wr;
k = k + 1;
end

% Write the data into Excel File
xlswrite('Data.xlsx',[array_excitation_frequency;...
array_rotor_speed;array_input;array_output;...
array_Vdssmag;array_Idssmag;angleVds;angleIds;...
array_Vqssmag;...
array_Iqssmag;angleVqs;angleIqs;...
array_inverter1;array_inverter2;array_efficiency]);
% Plot the Polar Plot of excitation conditions
plot1 = polar(angleVqs, array_Vqssmag/115,'*b');
hold on;
```

```
plot2 = polar(angleVds, array_Vdssmag/115,'*r');
hold on;
plot3 = polar(angleIds, array_Idssmag/5.2,'-r');
hold on;
plot4 = polar(angleIqs, array_Iqssmag/5.2,'-b');
set(plot3,'linewidth',2);
set(plot4,'linewidth',2);
```

Appendix G DYNAMIC SIMULATION CODE FOR VARIABLE FREQUENCY OPERATION

```
%%%%%%%%%%%%%%%%%%%%%%%%%%%%%%%%%%%%%%%%%%%%%%%%%%%%%%%%%%%%%%%%%%%%%%%%
% File Name: LineStartEquations.m
%%%%%%%%%%%%%%%%%%%%%%%%%%%%%%%%%%%%%%%%%%%%%%%%%%%%%%%%%%%%%%%%%%%%%%%%
% This file contains the machine equations
%%%%%%%%%%%%%%%%%%%%%%%%%%%%%%%%%%%%%%%%%%%%%%%%%%%%%%%%%%%%%%%%%%%%%%%%

function dy = LineStartEquations(t,y)

% Excitation Frequency at a chosen operating point
we = 380.7187;
% Rotor Frequency at a chosen operating point
wr = 400;

% Turns Ratio
Ndq = 1.18;
Nqd = 1/Ndq;

% Input Voltage at a chosen operating point
vqs = 104.2297*sqrt(2)*cos(we*t);
vds = 106.6269*sqrt(2)*cos(we*t+1.7089);

% Machine Resistances
rqs = 1.2;
rqr = 2.4;
rds = 7.5;
rdr = Ndq*Ndq*rqr;

% Inductances
Llqs = (3.74)/we;
Llqr = (2.17)/we;
```

```
Lmq = (42.46)/we;
Llds = (7.9652)/we;
Lldr = (3.0215)/we;
Lmd = (59.12)/we;
Lqs = Llqs + Lmq;
Lqr = Llqr + Lmq;
Lds = Llds + Lmd;
Ldr = Lldr + Lmd;

dy = zeros(4,1);
% Q Stator Winding Equation
dy(1) = vqs - rqs*((Lmq*y(2) - Lqr*y(1))...
/(Lmq^2 - Lqs*Lqr));
% D Stator Winding Equation
dy(2) = Nqd*wr*y(4) - rqr*((Lqs*y(2) - ...
Lmq*y(1))/(Lqs*Lqr - Lmq^2));
% Q Rotor Winding Equation
dy(3) = vds - rds*((Lmd*y(4) - Ldr*y(3))...
/(Lmd^2 - Lds*Ldr));
% D Rotor Winding Equation
dy(4) = - Ndq*wr*y(2) - rdr*((Lds*y(4) - ...
Lmd*y(3))/(Lds*Ldr - Lmd^2));
% y(1) = fqs
% y(2) = fqr
% y(3) = fds
% y(4) = fdr
% y(5) = wr
end


%%%%%%%%%%%%%%%%%%%%%%%%%%%%%%%%%%%%%%%%%%%%%%%%%%%%%%%%%%%%
% File Name: LineStartRunCode.m
%%%%%%%%%%%%%%%%%%%%%%%%%%%%%%%%%%%%%%%%%%%%%%%%%%%%%%%%%%%%
% This file initializes and calls the LineStart
% Equations.m and generate plots
%%%%%%%%%%%%%%%%%%%%%%%%%%%%%%%%%%%%%%%%%%%%%%%%%%%%%%%%%%%%
```

```
clc;
clear all;

% Excitation Frequency at a chosen operating point
we = 380.7187;

% Rotor Frequency at a chosen operating point
wr = 400;

% Turns Ratio
Ndq = 1.18;
Nqd = 1/Ndq;

% Machine Inductances
Llqs = (3.74)/we;
Llqr = (2.17)/we;
Lmq = (42.46)/we;
Llds = (7.9652)/we;
Lldr = (3.0215)/we;
Lmd = (59.12)/we;
Lqs = Llqs + Lmq;
Lqr = Llqr + Lmq;
Lds = Llds + Lmd;
Ldr = Lldr + Lmd;

yi1 = [0 0 0 0];% Initialization
[t1,y1] = ode45(@LineStart,[0 0.1],yi1);

% Current Calculation
iqs1 = (Lmq*y1(:,2) - Lqr*y1(:,1))/(Lmq^2 - Lqs*Lqr);
ids1 = (Lmd*y1(:,4) - Ldr*y1(:,3))/(Lmd^2 - Lds*Ldr);
% Voltages
vqs = 104.2297*sqrt(2)*cos(we*t1);
vds = 106.6269*sqrt(2)*cos(we*t1+1.7089);
% Power Calculation
Pem1 = vqs.*iqs1 + vds.*ids1;
```

```
% Plots

figure();

subplot(6,1,1)
plot(t1,(wr*60)/(4*pi)+t1*0,'k','LineWidth',1);
xlabel('Time');
title('Rotor Speed (RPM) (Fixed at 1909 PRM)');

subplot(6,1,2)
plot(t1,vqs/115,'LineWidth',1);
xlabel('Time');
title('Q Winding Voltage (RMS: 0.91 p.u.)');

subplot(6,1,3)
plot(t1,vds/115,'r','LineWidth',1);
xlabel('Time');
title('D Winding Voltage (RMS: 0.93 p.u.)');

subplot(6,1,4)
plot(t1,iqs1/5.2,'LineWidth',1);
xlabel('Time');
title('Q Winding Current (RMS: 0.91 p.u.)');

subplot(6,1,5)
plot(t1,ids1/5.2,'r','LineWidth',1);
xlabel('Time');
title('D Winding Current (RMS: 0.18 p.u.)');

subplot(6,1,6)
plot(t1,Pem1/248,'g','LineWidth',1);
xlabel('Time');
title('Power Output -1.24 p.u.');
```

REFERENCES

[1] Dudley, A. M. 1936. *Connecting induction motors*. 3rd ed. McGraw-Hill Book Company, Inc.

[2] Gasch, R., and J. Twele. 2002. *Wind power plants*. Berlin : Solarpraxis AG.

[3] Hrabovcova, V., L. Kalamen, P. Sekerak, and P. Rafajdus. 2010. Determination of single phase induction motor parameters. *Power Electronics Electrical Drives Automation and Motion (SPEEDAM), 2010 International Symposium on* 287 – 292.

[4] Krauss, P.C. 1965. Simulation of unsymmetrical 2-phase induction machines. *Power Apparatus and Systems, IEEE Transactions on* 84:1025 – 1037.

[5] Melendez-Vega, P. 2012. Design of tube-based blades and aluminum-foil-wound coils for human scale wind turbines. Master's thesis, University of Wisconsin - Madison.

[6] Monteiro, Joao P., Miguel R. Silvestre, Hugh Piggott, and Jorge C. Andre. 2013. Wind tunnel testing of a horizontal axis wind turbine rotor and comparison with simulations from two blade element momentum codes. *Journal of Wind Engineering and Industrial Aerodynamics* 123:99âŁ“106.

[7] Ojo, O., O. Omozusi, A. Ginart, and B. Gonoh. 1999. The operation of a stand-alone, single-phase induction generator using a single-phase, pulse-width modulated inverter with a battery supply. *Energy Conversion, IEEE Transactions on* 14:526 – 531.

[8] Piggott, Hugh. How to build a wind turbine, scotland 2005. http://www.scoraigwind.com/.

[9] Puchstein, A.F., and T.C. LLoyd. 1942. *Alternating-current machines*. 2nd ed. John Wiley and Sons, INC.

[10] Reed, J. 2008. Modeling of battery-charging wind turbines. Master's thesis, University of Wisconsin - Madison.

[11] Suhr, F.W. 1952. Toward an accurate evaluation of single-phase induction-motor constants. *Power Apparatus and Systems, Part III. Transactions of the American Institute of Electrical Engineers* 71:221–227.

[12] Van Der Merwe, C. et al. 1995. A study of methods to measure the parameters of single-phase induction motors. *Energy Conversion, IEEE Transactions on* 10:248 – 253.

[13] Veinott, Cyril G. 1948. *Fractional horsepower electric motors*. 2nd ed. McGraw-Hill Book Company.

[14] ———. 1959. *Theory and design of small induction motors*. McGraw Hill Book Company, INC.

[15] ———. 1970. *Fractional and sub-fractional horsepower electric motors*. 3rd ed. McGraw-Hill Book Company.